

Paleoenvironment of the Early Badenian (Middle Miocene) in the southern Vienna Basin (Austria) — multivariate analysis of the Baden-Sooss section

JOHANN HOHENEGGER¹, NILS ANDERSEN², KATALIN BÁLDI¹, STJEPAN ČORIĆ³,
PETER PERVESLER¹, CHRISTIAN RUPP³ and MICHAEL WAGREICH⁴

¹Department of Paleontology, University of Vienna, Althanstrasse 14, A-1090 Vienna, Austria; johann.hohenegger@univie.ac.at

²Leibniz Laboratory for Radiometric Dating and Stable Isotope Research, Christian-Albrechts-University, D-24118 Kiel, Germany

³Geological Survey of Austria, Neulinggasse 38, A-1030 Vienna, Austria

⁴Department of Geodynamics and Sedimentology, University of Vienna, Althanstrasse 14, A-1090 Vienna, Austria

(Manuscript received December 13, 2007; accepted in revised form June 12, 2008)

Abstract: Multivariate latent structure methods were used to determine environmental factors that influenced the distribution of magnetic susceptibility, calcium carbonate, organic carbon, stable oxygen and carbon isotopes, ichnofossils, calcareous nannoplankton and benthic as well as planktonic foraminifera in the 102 m long section of late Early Badenian age (Middle Miocene, Upper Lagenidae Zone) cored at Baden-Sooss for scientific investigations. Five factors ‘temperature’, ‘eutrophication’, ‘water stratification’, ‘oxygen-rich particulate organic material’ and ‘surface productivity’ controlled the variables to different degrees. The tectonically unaffected deeper part of the section (38 m to 102 m) started with a short warm period possibly characterizing environmental conditions of the preceding Lower Lagenidae Zone. A long ‘warm’ period from 78 m to 92 m followed the first temperature decline between 92 m and 100 m. Increased terrestrial input caused by intensified weathering through seasonal changes characterized warm periods. The subsequent long ‘colder’ period between 49 m and 78 m is distinguished by increased oxygen depletion, mixed water masses and dysoxic bottom conditions preferring carbonate and organic carbon production as well as inbenthic foraminifera. The following ‘warm’ period with decreasing oxygen depletion is abruptly finished between 36 m and 38 m in the sedimentary record through tectonic deformation. In the following period, ‘colder’ water conditions dominated interrupted by short warmer intervals, finally tending to warmer water at the top of the cored interval (8 m to 16 m). Although intermediate temperatures prevailed in the youngest period, oxygen depletion remained relatively high after obtaining the maximum in the previous period. This increase in oxygen depletion toward the top of the section is reflected in rising $\delta^{13}\text{C}$ isotope values together with decreasing temperatures, thus following — just after the Miocene ‘Monterey’ excursion — the slight global cooling trend between -14.7 and -13.9 Myr preceding the main Middle Miocene cooling period.

Key words: Miocene, Badenian, Vienna Basin, paleoenvironment, paleoclimate, multivariate analyses.

Introduction

A core was drilled for scientific investigations at the Badenian stratotype locality (Cicha et al. 1975; Papp & Steininger 1978), the former clay pit Baden-Sooss (Fig. 1), to shed light on the stratigraphic position and environmental conditions during sedimentation of the Middle Miocene “Badener Tegel” (Baden Group) using a multidisciplinary approach. Based on corresponding cycles in magnetic susceptibility, organic carbon and calcium carbonate content, correlation with orbital cycles was possible. Using the absence of the index fossil *Helicosphaera waltrans* and presence of the planktonic foraminifer *Orbulina universa* as stratigraphic tie points (Abdul Aziz et al. 2008), cross-correlations between orbital cycles and cycles in magnetic susceptibility enable precise dating of the section between -14.379 ± 0.001 and -14.142 ± 0.009 Myr (Hohenegger et al. 2008). The influence of environmental parameters obtained by investigations of magnetic susceptibility (Selge 2005), sedimentology, clay mineralogy and geochemistry (Wagreich et al. 2008), ichnology (Pervesler et al. 2008), paleoecology of benthic (Báldi & Hohenegger 2008) and

planktonic foraminifera (Rupp & Hohenegger 2008) together with calcareous nannoplankton (Čorić & Hohenegger 2008) is summarized and inter-correlated. Precise dating allows correlation with global climate changes (Zachos et al. 2001; Holbourn et al. 2007).

Environmental indicators

Several parameters dependent on environmental gradients could be defined in the Baden-Sooss section by detailed investigations. All these parameters were included in a comprehensive analysis to reconstruct the paleoenvironment during deposition of sediments in the Badenian Sea at the western border of the southern Vienna Basin. The following environmental variables were related to depth (age) in the section:

Anisotropic magnetic susceptibility (AMS)

Magnetic susceptibility was measured along the whole cored section at 5 cm spacing, resulting in 1797 measurements

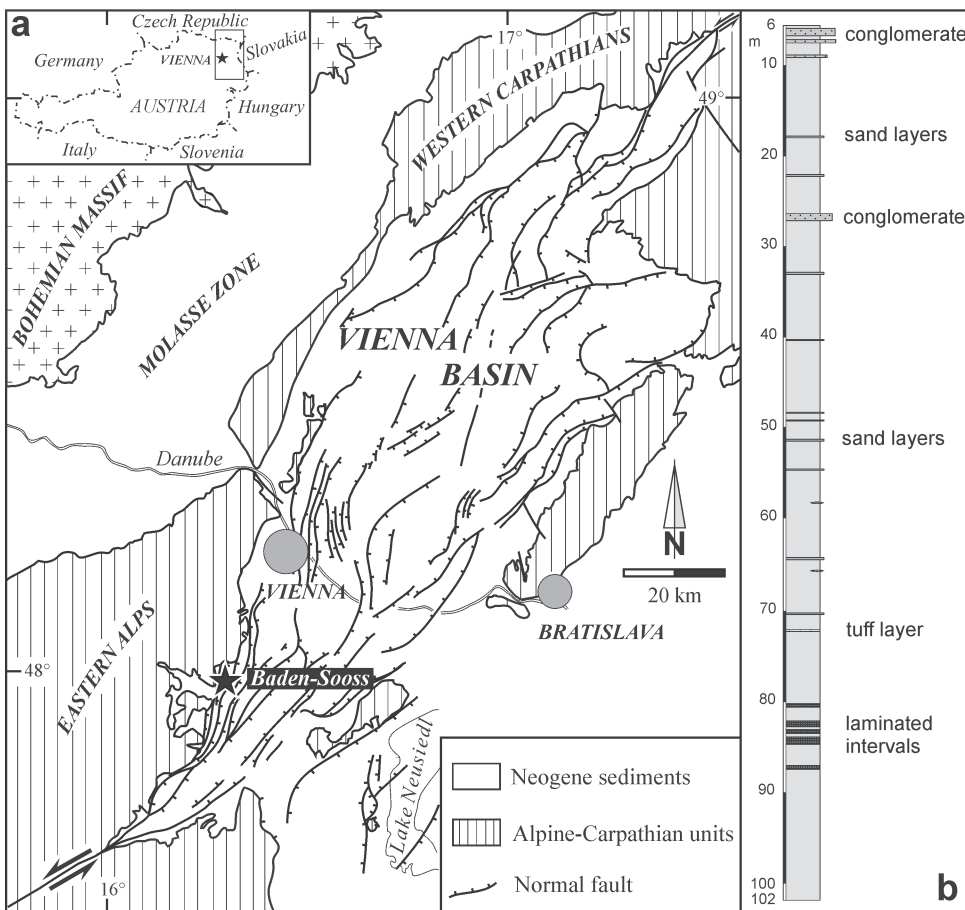


Fig. 1. **a** — Tectonic map of the Vienna Basin and location of the studied borehole Baden-Sooss. **b** — Schematic sedimentological log of the borehole Baden-Sooss (after Hohenegger et al. 2008).

(for details see Selge 2005; Wagreich et al. 2008). These measurements displayed significant periodic variations that could be decomposed into a set of four significant cycles with period lengths of 40 m, 23 m, 14 m and 11 m for the tectonically unaffected part of the section from 40 m to 102 m (Hohenegger et al. 2008: fig. 5). The high negative correlation with CaCO_3 and organic carbon (Hohenegger et al. 2008: table 1) together with similar period numbers and lengths of the three variables (Hohenegger et al. 2008: fig. 5) led to the idea of comparing the four significant period lengths with orbital cycles. Correlation between different sequences of orbital cycles and the three cycles of magnetic susceptibility, CaCO_3 and organic carbon at Baden-Sooss indicates that they correspond with the 100 kyr eccentricity, 41 kyr obliquity, 23 kyr and 19 kyr precession cycles (Hohenegger et al. 2008: table 3).

The major variations of magnetic susceptibility can be found through combining the four decomposed sinusoidal functions into a compound function (Fig. 2a). This function shows a clear differentiation of the upper (6 m to 40 m) from the deeper part of the cored section (40 m to 102 m). Period lengths are shorter in the upper part and distances between the three main peaks differ significantly (Fig. 2a). Shorter periods in the upper part of the sequence are caused by the loss of section through tectonic deformation recognizable as small-scale fault planes (Wagreich et al. 2008). The three main peaks in magnetic susceptibility are equated with orbital 100 kyr eccentricity peaks. They result from a higher input

of detrital magnetic components, i.e. hematite, through seasonal differences, caused by increased eccentricity and obliquity influencing solar radiation (insolation), precipitation, evaporation and wind systems (Selge 2005). Although oscillations in magnetic susceptibility are intensified in the upper part of the section showing higher amplitudes (Fig. 2a), the mean level is significantly lower than in the deeper part of the section (Hohenegger et al. 2008: table 2). This can be interpreted as a generally higher, but less varying sedimentary input in the deeper part of the section. While the rate of sedimentary input was on average lower in the upper part of the section, it was intensive during periods of detritus input (Fig. 2a). The lower mean susceptibility is also documented in the significant correlation with age as expressed by depth in the cored sequence (Table 1).

Calcium carbonate

Percentages of CaCO_3 were measured in the tectonically unaffected deeper part of the section (40 m to 102 m) in 20 cm intervals, resulting in 310 measurements (Khatun 2007). Twenty-two overview samples were taken including six samples for the upper part of the section between 6 m and 40 m (Fig. 2b). Oscillations in the deeper part of the section could be decomposed into four sinusoidal functions with period lengths identical to those of magnetic susceptibility and organic carbon (Fig. 2b). The high negative correlation be-

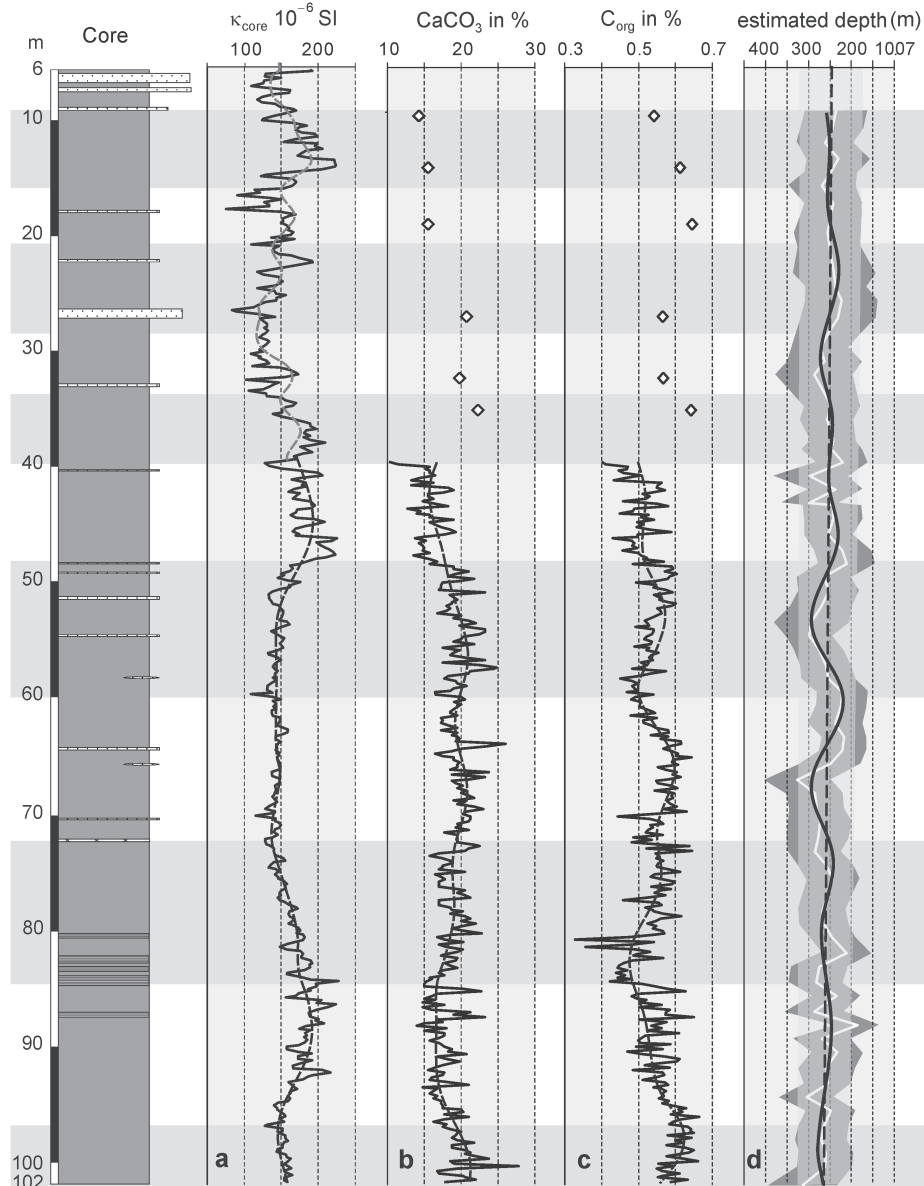


Fig. 2. a — Magnetic susceptibility, fit by sinusoidal regression based on power spectra. b — Percentages of calcium carbonate, fit by sinusoidal regression based on power spectra. c — Percentages of organic carbon, fit by sinusoidal regression based on power spectra. d — Estimated water depth, 95% confidence intervals, fit by linear regression and by sinusoidal regression based on power spectra. Grey and white bands indicate periods obtained by moving averages of magnetic susceptibility.

tween calcium carbonate and magnetic susceptibility supports the idea of an opposite reaction to environmental conditions (Hohenegger et al. 2008). During periods of high detrital sedimentary input expressed in peaks of magnetic susceptibility, calcium carbonate content as a result of shell production (mainly planktonic and benthic foraminifera and calcareous nannoplankton) is low (Wagreich et al. 2008). Productivity of planktonic organisms is high in colder water indicating that peaks in calcium carbonate coincide with minima in orbital eccentricity and obliquity (Hohenegger et al. 2008). Although calcium carbonate content varies oppositely to magnetic susceptibility intensity, it also shows a significant decrease from the lower to the upper part of the section (Table 1).

Organic carbon

The sample set used for the investigation of calcium carbonate was also used to measure percentages of organic carbon (Khatun 2007). The organic carbon content is low throughout the entire section (Fig. 2c) decreasing upwards (Table 1; Wagreich et al. 2008). Periods of oscillation coincide between organic carbon and CaCO_3 (Fig. 2c) but with a significant 3.2 m phase difference to CaCO_3 (Hohenegger et al. 2008: fig. 6). Although correlation with magnetic susceptibility is negative, it is less significant than CaCO_3 due to the later onset of periods, e.g. phase differences (Hohenegger et al. 2008: table 1). Similar to magnetic susceptibility and CaCO_3 the decrease of organic carbon content with time is significant (Table 1).

Table 1: Correlation matrix (Pearson's correlation coefficients) between environmental variables of the complete core. Significant correlations marked by grayish background.

		δ ¹⁸ O Uvigerina grilli												
		δ ¹³ C Uvigerina grilli						δ ¹⁸ O Uvigerina elegans						
		δ ¹³ C Hoeglundina elegans			δ ¹⁸ O Hoeglundina elegans			δ ¹³ C Uvigerina elegans			δ ¹⁸ O Uvigerina elegans			
core depth		correlation	1	-0.156	-0.159	-0.275	-0.387	0.262	0.179	0.517	0.779	0.467	-0.393	0.315
magnetic susceptibility		significance number	479	0.000	0.002	0.000	0.004	0.014	0.067	0.150	0.003	0.000	0.026	0.063
calcium carbonate		correlation significance number	478	478	1	-0.457	-0.236	-0.186	0.013	-0.259	-0.083	-0.309	-0.442	-0.355
organic carbon		correlation significance number	316	316	316	0.000	0.000	0.106	0.457	0.015	0.341	0.058	0.000	0.020
hydrogen index		correlation significance number	316	316	316	0.407	1	0.387	0.027	0.025	-0.720	-0.478	0.034	0.288
δ ¹³ C Globigerinoides trilobus		correlation significance number	71	71	71	-0.016	0.027	0.087	1	0.103	0.559	0.114	0.305	0.390
δ ¹⁸ O Globigerinoides trilobus		correlation significance number	71	71	51	0.455	0.425	0.291	0.291	0.196	0.003	0.303	0.006	0.001
δ ¹³ C Globigerinoides bulliformis		correlation significance number	71	71	51	-0.083	-0.028	-0.720	-0.720	0.467	0.534	0.576	0.823	0.662
δ ¹⁸ O Globigerinoides bulliformis		correlation significance number	71	71	51	0.207	0.259	0.258	0.025	0.103	0.103	0.103	0.323	0.522
δ ¹³ C Hoeglundina elegans		correlation significance number	73	73	53	-0.442	-0.446	-0.478	(a)	0.114	0.534	0.226	0.272	0.422
δ ¹⁸ O Hoeglundina elegans		correlation significance number	25	25	6	-0.355	0.263	0.288	0.099	0.390	0.576	0.706	0.721	0.706
δ ¹³ C Uvigerina grilli		correlation significance number	73	73	53	0.001	0.028	0.018	0.034	0.305	0.490	0.272	0.721	0.758
δ ¹⁸ O Uvigerina grilli		correlation significance number	25	25	6	-0.413	0.907	0.017	-	0.244	0.823	0.323	0.960	0.720
Δδ ¹⁸ O		correlation significance number	69	69	50	0.020	0.006	0.487	-	0.137	0.000	0.067	0.000	0.002
core depth		magnetic susceptibility	479	478	1	-0.156	-0.159	-0.275	-0.387	0.262	0.179	0.517	0.779	0.467
calcium carbonate		significance number	479	478	316	0.000	0.002	0.000	0.004	0.014	0.067	0.150	0.003	0.026
organic carbon		significance number	316	316	316	-0.457	-0.236	-0.186	0.013	-0.259	-0.083	-0.309	-0.442	-0.355
hydrogen index		significance number	316	316	316	0.000	0.000	0.106	0.457	0.015	0.341	0.058	0.000	0.020
δ ¹³ C Globigerinoides trilobus		significance number	47	47	47	0.405	0.455	0.455	0.455	0.455	0.455	0.455	0.455	0.455
δ ¹⁸ O Globigerinoides trilobus		significance number	47	47	47	0.004	0.004	0.004	0.004	0.004	0.004	0.004	0.004	0.004
δ ¹³ C Globigerinoides bulliformis		significance number	71	71	51	-0.016	0.013	0.013	0.013	0.013	0.013	0.013	0.013	0.013
δ ¹⁸ O Globigerinoides bulliformis		significance number	71	71	51	0.457	0.457	0.457	0.457	0.457	0.457	0.457	0.457	0.457
δ ¹³ C Hoeglundina elegans		significance number	73	73	53	-0.355	-0.442	-0.446	-0.478	(a)	0.114	0.534	0.226	0.272
δ ¹⁸ O Hoeglundina elegans		significance number	25	25	6	-0.355	0.263	0.288	0.099	0.390	0.576	0.706	0.721	0.758
δ ¹³ C Uvigerina grilli		significance number	73	73	53	0.001	0.028	0.018	0.034	0.305	0.490	0.272	0.721	0.758
δ ¹⁸ O Uvigerina grilli		significance number	25	25	6	-0.413	0.907	0.017	-	0.137	0.000	0.067	0.000	0.002
Δδ ¹⁸ O		significance number	69	69	50	0.020	0.006	0.487	-	0.137	0.000	0.067	0.000	0.002

Table 1: Continued from the previous pages.

		Coccolithus pelagicus										reworked nanoplankton										
		ichnofabric type 6					ichnofabric type 1					ichnofabric type 6					ichnofabric type 1					
		older water planktonic foraminifera					warm water planktonic foraminifera					abundance planktonic foraminifera					diversity planktonic foraminifera					
water depth																						
core depth	correlation significance number	-0.249 0.024	0.528 0.000	-0.255 0.014	0.290 0.006	-0.442 0.471	0.013 0.002	-0.468 0.169	-0.165 0.086	-0.232 0.000	0.319 0.000	0.179 0.000	0.346 0.000	0.558 0.000								
magnetic susceptibility	correlation significance number	-0.113 0.190	-0.150 0.101	0.512 0.000	-0.464 0.015	0.253 0.011	0.380 0.000	-0.568 0.000	0.552 0.000	-0.567 0.000	-0.234 0.008	0.126 0.000	-0.347 0.000	0.118 0.119								
calcium carbonate	correlation significance number	-0.022 0.441	-0.156 0.128	-0.092 0.252	0.310 0.011	0.052 0.352	-0.175 0.187	0.091 0.042	-0.332 0.253	0.223 0.127	-0.260 0.091	0.270 0.083	-0.116 0.032	0.286 0.000	-0.003 0.489	-0.293 0.006						
organic carbon	correlation significance number	-0.064 0.337	-0.038 0.392	0.250 0.033	0.099 0.236	0.091 0.253	-0.332 0.042	0.223 0.177	-0.233 0.127	-0.260 0.091	0.270 0.083	-0.116 0.032	0.286 0.000	-0.003 0.489	-0.293 0.006							
hydrogen index	correlation significance number	0.054 0.375	-0.047 0.388	0.149 0.183	0.156 0.171	0.241 0.070	-0.544 0.005	0.267 0.121	-0.317 0.080	0.454 0.019	-0.296 0.036	0.283 0.042	-0.294 0.135	0.283 0.046	-0.435 0.16							
$\delta^{13}\text{C}$ <i>Globigerinoides trilobus</i>	correlation significance number	-0.178 0.088	-0.153 0.131	-0.169 0.106	0.101 0.230	-0.169 0.106	-0.303 0.062	-0.176 0.190	-0.137 0.247	-0.194 0.166	-0.194 0.302	0.258 0.25	0.210 0.194	0.114 0.321								
$\delta^{18}\text{O}$ <i>Globigerinoides trilobus</i>	correlation significance number	-0.076 0.283	0.005 0.486	-0.467 0.000	0.208 0.062	-0.490 0.000	-0.132 0.256	0.389 0.022	-0.571 0.022	0.467 0.007	0.500 0.000	0.132 0.162	0.018 0.472	-0.250 0.151								
$\delta^{13}\text{C}$ <i>Globigerina bulloides</i>	correlation significance number	-0.160 0.250	0.027 0.457	-0.036 0.442	0.094 0.351	-0.319 0.091	-0.682 0.068	0.674 0.071	-0.093 0.430	0.206 0.348	0.018 0.467	0.007 0.487	0.520 0.145	-0.411 0.209								
$\delta^{18}\text{O}$ <i>Globigerina bulloides</i>	correlation significance number	-0.180 0.224	-0.371 0.059	0.461 0.024	-0.568 0.024	-0.337 0.006	0.807 0.257	-0.862 0.014	0.726 0.011	0.463 0.292	0.118 0.025	0.812 0.321	-0.094 0.430									
$\delta^{13}\text{C}$ <i>Hoeglundina elegans</i>	correlation significance number	-0.114 0.197	0.619 0.000	-0.637 0.000	0.451 0.000	-0.638 0.000	-0.388 0.021	-0.038 0.424	-0.472 0.006	0.174 0.188	0.336 0.003	0.189 0.067	0.427 0.027	0.348 0.061								
$\delta^{18}\text{O}$ <i>Hoeglundina elegans</i>	correlation significance number	-0.370 0.059	-0.545 0.371	0.388 0.062	-0.775 0.062	-0.561 0.062	-0.534 0.095	0.845 0.108	-0.539 0.106	-0.073 0.374	-0.251 0.130	0.852 0.076	-0.632 0.089									
$\delta^{13}\text{C}$ <i>Uvigerina grilli</i>	correlation significance number	-0.592 0.004	-0.206 0.214	-0.315 0.109	0.028 0.457	-0.515 0.017	-0.617 0.070	0.653 0.056	-0.214 0.322	0.305 0.253	-0.071 0.376	0.098 0.331	0.533 0.138	0.130 0.403								
$\delta^{18}\text{O}$ <i>Uvigerina grilli</i>	correlation significance number	-0.151 0.131	-0.288 0.017	-0.223 0.052	0.051 0.358	-0.090 0.259	0.196 0.168	0.368 0.032	-0.205 0.157	0.244 0.115	0.432 0.000	-0.155 0.128	-0.081 0.374	-0.489 0.020								
$\Delta\delta^{18}\text{O}$		57	54	54	54	54	54	54	54	26	26	56	56	18								

Table 1: *Continued from the previous pages.*

In the deeper part of the section, high organic carbon content comes mainly from terrestrial plant material as is shown by Rock Eval pyrolysis. The Hydrogen Index (HI; Espitalié et al. 1977) is low and more typical of type III kerogen (Wagreich et al. 2008). Correspondence of HI with the organic carbon cycle (Table 1) corroborates the increase of organic carbon originating from marine photosynthetic organisms during periods of high productivity.

Paleowater-depth

Estimation of paleowater-depth is based on foraminifera and performed in two ways. First, the Plankton/Benthos-ratio in the modified form of Van der Zwaan et al. (1990) was used to estimate the depth in meters (Báldi & Hohenegger 2008). This method indicates that the water depth oscillated strongly in the deeper part of the section. The average water depth would have been around -600 m, with a minimum of -211 m and a maximum of -863 m. In the upper part of the section there would have been a strong shallowing to -117 m water depth at 10 m in the section core depth, suddenly sinking to -404 m water depth at 8.4 m (see Báldi & Hohenegger 2008: fig. 2a). These oscillations of inferred water depth are at least partly an artefact of the restricted ecological conditions of the shallow and marginal Badenian Sea, e.g. cold water ingressions leading to a strong increase in planktonic foraminiferal numbers. Their abundance is strongly correlated with the estimates of water depth ($r=0.98$; $p(t_0)=2.58E-53$). We conclude that depth estimation of the Badenian Sea in the Vienna Basin using the method of Van der Zwaan et al. (1990) is biased and is merely a reflection of plankton abundance during cooler periods.

For paleowater-depth estimate we used the method of Hohenegger (2005) based on depth ranges of benthic foraminifera and extended by the inclusion of species abundance

$$\text{depth} = \sum_{j=1}^{j=k} [(l_j \cdot n_j)/d_j] / \sum_{j=1}^{j=k} (n_j/d_j)$$

where l_j is the geometric mean of the distribution borders, d_j the depth range and n_j the abundance of the j^{th} species (see Báldi & Hohenegger 2008). This transfer function depends on depth ranges of benthic species, which for extant species are based on modern ranges and for extinct species estimated by comparison with ranges of the morphologically most related living species. This estimate must not be understood as point estimation, but represent intervals within 95% confidence limits (Hohenegger 2005). Diversity, abundance or species number of benthic foraminifera could also influence the estimated depth gradients. Testing dependencies by multiple regression confirms the highly significant independence of this method from the variables abundance, species number and diversity.

Power spectral analysis demonstrates significant oscillations [$p(\text{random}) = 0.0066$] in these depth estimations (Hammer & Harper 2005). Therefore, they could be fitted by sinusoidal regression (Fig. 2d). Since independence of this estimation from benthos diversity and abundance has been tested, these oscillations can be interpreted as sea-level changes with a maximum difference of 75 m (Fig. 2d).

Additionally, linear regression was used to test for dependence on depth (age) in the section. The regression

$$\text{mean water depth} = 0.201 \cdot \text{core depth} - 244.41$$

indicates a significant [$p(t_0) = 0.0334$] decrease in water-depth related to depth in the stratigraphic sequence. Figure 1d shows the confidence interval (-206 m to -323 m water depth) at the deepest sample (102 m) shallowing to an interval width from -172 m to -320 m water depth at the highest sample (8 m). The mean trend of water depth in the section is from -265 m to -246 m, indicating a weak but significant shallowing tendency of +19 m (Fig. 2d).

Stable isotopes

The tests of planktonic and benthic foraminifera from 78 samples were used to obtain $\delta^{18}\text{O}$ - and $\delta^{13}\text{C}$ -ratios. Stable isotopes were measured on *Globigerinoides trilobus*, a typical warm water planktonic foraminifer (Li et al. 1999). It is abundant in the deeper part of the section, becoming rare in the upper part. Therefore, additional measurements were performed on the abundant *Globigerina bulloides* in samples from the upper part of the section that indicate cooler waters (Rupp & Hohenegger 2008). *Hoeglundina elegans*, an epibenthic foraminifer with an aragonite test was used to determine the stable isotope composition of bottom water. When preserved, aragonite tests show the original isotope composition of the surrounding water, while calcite of fossil tests can be affected by even weak diagenesis altering the oxygen isotope composition (Sharp 2007). Comparing $\delta^{18}\text{O}$ isotopes of the aragonite and calcite test walls, enrichment relative to the equilibrium value for calcite has been noticed (Grossmann 1984). Because *H. elegans* is rare in the upper part of the section as a result of the strong increase of inbenthic foraminifera, stable isotopes were also measured on the inbenthic *Uvigerina grilli*. Here, $\delta^{13}\text{C}$ ratios are influenced by the microhabitat, where the decomposition of sedimentary organic matter correlated to sediment depth and food supply leads to depletion of $\delta^{13}\text{C}$ (e.g. Rohling & Cooke 1999).

Oxygen isotopes

The $\delta^{18}\text{O}$ of *G. trilobus* significantly increases (Table 2) in the deeper part of the section from -1.82 at 102 m to -1.32 at 40 m (Fig. 3a) demonstrating minor oscillations (residuals = 0.28) that are negatively correlated with magnetic susceptibility (Table 2). $\delta^{18}\text{O}$ -values are stable in the upper part of the section, varying with a standard deviation (SD) of 0.35 around the mean of -1.61. Negative correlations with magnetic susceptibility are close to being significant (Table 2). Oxygen isotopes in *G. bulloides* behave dissimilarly to *G. trilobus* in the upper part of the section (Fig. 3a). Starting with low values of -1.85 at 40 m depth that are close to those of *G. trilobus* (-1.94), a rapid increase to 0.61 at 34.8 m is followed by oscillations (SD=0.22) around a mean of 0.64 (Fig. 3a). The high correlation between $\delta^{18}\text{O}$ -values of both planktonic species is evident in their parallel fluctuations (Fig. 3a). Both vary with magnetic susceptibility (Table 2).

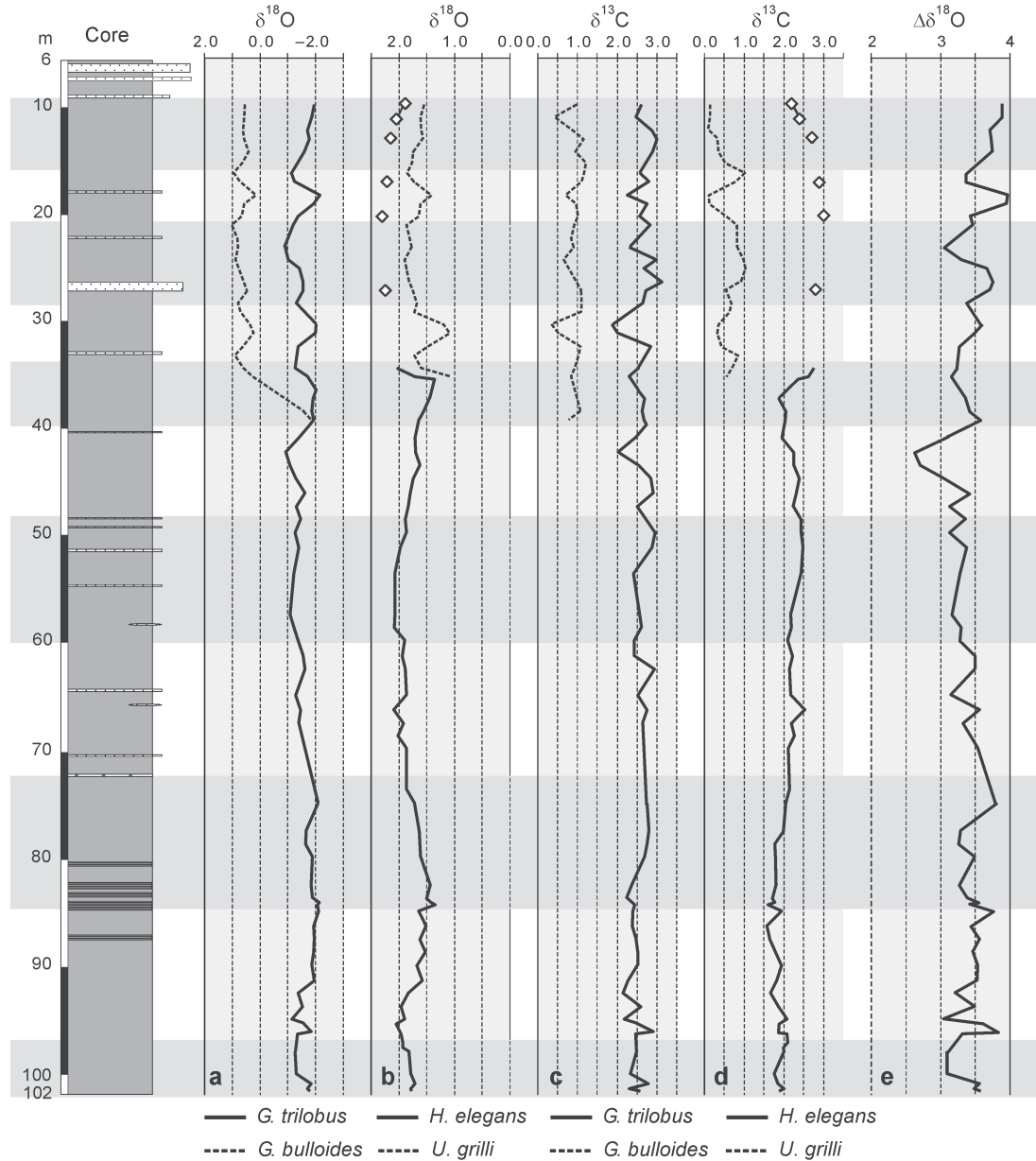


Fig. 3. a — Stable oxygen isotopes of planktonic foraminifera. b — Stable oxygen isotopes of benthic foraminifera. c — Stable carbon isotopes of planktonic foraminifera. d — Stable carbon isotopes of benthic foraminifera. e — Absolute differences in stable oxygen isotopes between planktonic and benthic foraminifera. Grey and white bands indicate periods obtained by moving averages of magnetic susceptibility.

The strong difference but parallel reaction in $\delta^{18}\text{O}$ may be interpreted as an ontogenetic effect in *G. bulloides* (Kroon & Darling 1995), because juveniles of that species calcify in deeper water and later migrate to shallower waters (Spero & Lea 1996; Bemis et al. 1998). However, more recent isotope investigations indicate a deeper habitat of *G. bulloides* throughout its life cycle (Chiessi et al. 2007). Thus the coincidence of $\delta^{18}\text{O}$ -values in *G. trilobus* and *G. bulloides* at 40 m could be the result of mixed water masses, as is suggested by the high $\delta^{18}\text{O}$ of -0.92 in *G. trilobus* at 42 m (Fig. 2e).

Oxygen isotopes of the epibenthic *H. elegans* demonstrate an independence from depth in the deeper part of the section (Table 2), weakly varying ($SD=0.223$) around a mean of 1.81. In this part of the section, oscillations of the $\delta^{18}\text{O}$ are

highly negatively correlated with magnetic susceptibility (Table 2; Fig. 2b). After a strong increase between 40 m and 35 m, the few $\delta^{18}\text{O}$ measurements are close to the mean value of 2.13 ($SD=0.14$). According to the few measurements in the upper part of the section, the negative correlation ($r=-0.357$) with magnetic susceptibility is insignificant (Table 2). For a better resolution of benthic $\delta^{18}\text{O}$ in the upper part of the section, stable isotopes were measured on the inbenthic species *U. grilli*. Regression analysis of $\delta^{18}\text{O}$ between *U. grilli* and *H. elegans* confirms a linear relationship. The 95% confidence interval for the slope of the regression ($b=0.947$) includes the value of 1 which would indicate identical relations, while the intercept of 0.582 falls within the confidence limits of $0.78+19\text{‰}$ for enriched ^{18}O in aragonite

Table 2: Correlation matrix (Pearson's correlation coefficients) between environmental variables of the deeper core (lower left triangle matrix) and the upper core (upper right triangle matrix). Significant correlations marked by grayish background.

Table 2: *Continued.*

Table 2: Continued from the previous pages.

	water depth	inherent foraminifera	oxyphyle foraminifera	abundance benthic foraminifera	diversity benthic foraminifera	abundance planktonic foraminifera	diversity planktonic foraminifera	warm water planktonic foraminifera	colder water planktonic foraminifera	ichnofabric type 1	ichnofabric type 6	Coccolithus pelagicus	reworked nannoplankton	
core depth	correlation significance number	-0.175 0.212	0.397 0.027	0.260 0.110	0.144 0.251	0.079 0.357	-0.027 0.468	-0.232 0.478	0.019 0.378	-0.106 0.000	0.351 0.000	0.528 0.488	0.005 0.007	
magnetic susceptibility	correlation significance number	-0.077 0.363	-0.312 0.069	0.619 0.001	-0.681 0.000	0.677 0.133	0.368 0.002	-0.789 0.001	0.817 0.002	-0.787 0.001	-0.288 0.000	0.529 0.000	-0.302 0.044	0.344 0.025
calcium carbonate	correlation significance number	-0.579 0.114	-0.458 0.219	0.116 0.426	0.850 0.034	-0.317 0.302	-0.998 0.020	-0.320 0.396	-0.031 0.490	-0.135 0.457	0.085 0.428	-0.113 0.405	-0.891 0.150	0.059 0.481
organic carbon	correlation significance number	-0.720 0.053	-0.541 0.173	0.841 0.037	0.375 0.267	0.288 0.319	-0.998 0.019	-0.202 0.435	-0.153 0.451	-0.013 0.496	0.148 0.376	0.611 0.073	-0.966 0.084	-0.148 0.453
hydrogen index	-	-	-	-	-	-	-	-	-	-	-	-	-	-
$\delta^{13}\text{C}$ <i>Globigerinoides trilobus</i>	correlation significance number	-0.388 0.037	0.033 0.447	0.006 0.490	-0.063 0.399	-0.250 0.151	-0.605 0.056	0.304 0.232	0.111 0.396	0.169 0.344	-0.062 0.386	0.263 0.107	0.377 0.266	0.316 0.302
$\delta^{18}\text{O}$ <i>Globigerinoides trilobus</i>	correlation significance number	-0.278 0.105	0.199 0.207	-0.435 0.031	0.500 0.015	-0.760 0.000	-0.171 0.342	0.662 0.037	-0.483 0.112	0.365 0.187	0.182 0.198	-0.033 0.439	0.711 0.089	0.337 0.290
$\delta^{13}\text{C}$ <i>Globigerina bullides</i>	correlation significance number	-0.160 0.250	0.027 0.457	-0.036 0.442	0.094 0.351	-0.319 0.091	-0.682 0.068	0.674 0.071	-0.093 0.430	0.206 0.348	0.018 0.467	0.007 0.487	0.520 0.145	-0.411 0.209
$\delta^{18}\text{O}$ <i>Globigerina bullides</i>	correlation significance number	0.180 0.224	0.690 0.001	-0.371 0.059	0.461 0.024	-0.568 0.006	-0.337 0.257	0.807 0.026	-0.862 0.014	0.726 0.057	0.463 0.011	0.118 0.292	0.812 0.025	-0.094 0.430
$\delta^{13}\text{C}$ <i>Hoeglundina elegans</i>	correlation significance number	-0.113 0.312	0.489 0.017	-0.556 0.007	0.533 0.009	-0.801 0.000	-0.610 0.054	0.797 0.009	-0.716 0.023	0.749 0.016	0.391 0.024	-0.081 0.346	0.787 0.032	-0.638 0.086
$\delta^{18}\text{O}$ <i>Hoeglundina elegans</i>	correlation significance number	-0.207 0.198	0.574 0.010	-0.311 0.120	0.382 0.072	-0.695 0.001	-0.396 0.218	0.523 0.143	-0.502 0.155	0.602 0.103	0.393 0.035	0.116 0.304	0.643 0.278	0.998 0.018
$\delta^{13}\text{C}$ <i>Uvigerina grilli</i>	correlation significance number	-0.370 0.059	-0.086 0.371	-0.545 0.012	0.388 0.062	-0.775 0.000	-0.561 0.095	0.845 0.008	-0.534 0.108	0.539 0.106	-0.073 0.374	-0.251 0.130	0.852 0.016	-0.632 0.089
$\delta^{18}\text{O}$ <i>Uvigerina grilli</i>	correlation significance number	-0.592 0.004	-0.206 0.214	-0.315 0.109	0.028 0.457	-0.515 0.017	-0.617 0.070	0.653 0.056	-0.214 0.253	0.305 0.253	-0.071 0.376	0.098 0.331	0.533 0.138	0.130 0.403
$\Delta\delta^{18}\text{O}$	correlation significance number	-0.209 0.189	-0.266 0.151	-0.327 0.100	0.247 0.169	-0.398 0.057	0.228 0.311	0.351 0.220	-0.098 0.417	-0.112 0.406	-0.239 0.142	-0.259 0.122	-0.161 0.420	-0.569 0.216

Table 2: *Continued from the previous pages.*

compared to calcite tests (Grossmann 1984). *Uvigerina grilli* does not show dependency of $\delta^{18}\text{O}$ from depth in the section (Table 2) but weak variations ($SD=0.23$) around the mean of 1.62. The obvious periods in *U. grilli* $\delta^{18}\text{O}$ do not correlate with magnetic susceptibility (Table 2).

Carbon isotopes

Stable carbon isotopes in *G. trilobus* demonstrate a weak but significant increase from the bottom to the top of the sequence (Fig. 3c). In the deeper part, the increase starts with 2.48 at 102 m and ends with 2.66 at 40 m. Variability is not large (residuals: 0.21) and the periodicity is close to having a significant negative correlation with magnetic susceptibility (Table 2). Carbon isotopes of *G. trilobus* do not show any relation to depth in the upper part, but values vary more ($SD=0.29$) around the mean of 2.63 compared to the deeper part (Fig. 3c). The positive correlation of $\delta^{13}\text{C}$ oscillations with periods in magnetic susceptibility is significant in this part of the section (Table 2). $\delta^{13}\text{C}$ -values of *G. bulloides* exhibit similar variability ($SD=0.24$) around a mean value of 0.91, which is much lower than that of *G. trilobus* (Fig. 3c). The correlation in $\delta^{13}\text{C}$ between both planktonic species is significant, the result of parallel fluctuations (Fig. 3c). The large differences between the $\delta^{13}\text{C}$ of *G. trilobus* and *G. bulloides* may result from their different habitats (Chiessi et al. 2007).

Carbon isotopes of *H. elegans* are distinguished by a significant increase in the deeper part of the section (Table 2) starting with 1.81 at 102 m and reaching 2.37 at 40 m. Variations are weak (residuals: 0.17) and correlate negatively with magnetic susceptibility (Fig. 3d; Table 2). The few measurements in the upper part of the section do not define a trend, but hint at strong variability ($SD=0.28$) around a mean value of 2.68. Although there are only a few measurements in the upper part, the negative correlation with magnetic susceptibility is significant (Table 2). This tendency is confirmed by the inbenthic *U. grilli* for which there are more measurements. The linear relations in $\delta^{13}\text{C}$ between *H. elegans* and *U. grilli* shows a significant slope of the regression line ($b=0.892$) and the 95% confidence limit includes the coefficient of 1 for identical relations. A constant difference of -1.92 between *H. elegans* and *U. grilli* is shown by the intercept of the regression line. As mentioned above, it has been found that pore water gradients of $\delta^{13}\text{C}$ decrease with sediment depth due to decomposition of sedimentary organic matter and by the amount of carbon used as a food supply (Rohling & Cooke 1999). As indicated for *H. elegans*, constancy of carbon isotope

Factor	Explained variance initial eigenvalue			Sum of squared factor loadings			% of variance after rotation
	Total	% of variance	Cumulative %	Total	% of variance	Cumulative %	
1	6.12	30.6	30.6	4.7	23.4	23.4	34.9
2	2.89	14.5	45.1	2.1	10.7	34.1	3.2
3	2.40	12.0	57.1	2.9	14.4	48.5	24.1
4	1.57	7.8	64.9	1.3	6.3	54.7	3.3
5	1.16	5.8	70.7	1.1	5.6	60.3	4.7
6	0.99	5.2	75.9				
7	0.86	4.3	80.3				
8	0.75	3.7	84.1				
9	0.55	2.8	86.8				
10	0.49	2.5	89.3				
11	0.40	2.0	91.3				
12	0.35	1.8	93.1				
13	0.29	1.4	94.5				
14	0.28	1.4	95.9				
15	0.24	1.2	97.1				
16	0.19	0.9	98.0				
17	0.16	0.8	98.9				
18	0.13	0.7	99.5				
19	0.07	0.3	99.9				
20	0.03	0.1	100.0				

Table 3a

Table 3b	Factor loadings				
	1	2	3	4	5
colder water planktonic foraminifera	0.806	-0.142	0.228	-0.483	
diversity planktonic foraminifera	-0.803	0.302		-0.239	
abundance planktonic foraminifera	0.793			-0.222	-0.129
magnetic susceptibility	-0.662	0.119	-0.167	0.102	
calcium carbonate	0.657				
reworked nannoplankton	-0.405	-0.167	0.132	0.211	-0.115
$\delta^{18}\text{O}$ <i>Globigerinoides trilobus</i>		1.007		0.314	
$\Delta\delta^{18}\text{O}$	0.112	-0.871	0.288		0.214
ichnofabric type 1		0.588	0.245		
$\delta^{13}\text{C}$ <i>Hoeglundina elegans</i>	-0.135	0.196	0.786	0.165	
inbenthic foraminifera	-0.162	-0.124	0.675		
abundance benthic foraminifera	0.113		0.662		
<i>Coccolithus pelagicus</i>			0.558		
$\delta^{18}\text{O}$ <i>Hoeglundina elegans</i>		0.389	0.528	0.471	0.208
ichnofabric type 6	-0.230		-0.147	0.772	
organic carbon	0.250			0.481	
warm water planktonic foraminifera	-0.350	-0.121	-0.342	-0.283	0.596
$\delta^{13}\text{C}$ <i>Globigerinoides trilobus</i>				0.231	0.523
diversity benthic foraminifera		-0.116	-0.240		
oxyphylic foraminifera	-0.221	-0.185	-0.246	0.228	

Table 3c	Factor loadings				
	1	2	3	4	5
colder water planktonic foraminifera	0.847	0.160	0.373	0.218	-0.604
diversity planktonic foraminifera	0.814	0.394	0.282	-0.285	-0.345
abundance planktonic foraminifera	-0.726	-0.199	-0.638	-0.307	0.565
magnetic susceptibility	-0.724	-0.184	-0.527		0.176
calcium carbonate	-0.689		-0.443	-0.389	
reworked nannoplankton	0.598	0.211	0.266		
$\delta^{18}\text{O}$ <i>Globigerinoides trilobus</i>	-0.363	-0.361	-0.108	0.231	
$\Delta\delta^{18}\text{O}$	0.363	0.927	0.316		0.159
ichnofabric type 1		-0.780	0.184	0.373	0.145
$\delta^{13}\text{C}$ <i>Hoeglundina elegans</i>	0.256	0.609	0.290	-0.130	0.140
inbenthic foraminifera	0.365	0.277	0.883	0.359	0.251
abundance benthic foraminifera	0.475	0.389	0.740	0.499	0.328
<i>Coccolithus pelagicus</i>	0.166		0.648	0.261	0.144
$\delta^{18}\text{O}$ <i>Hoeglundina elegans</i>	0.498	0.227	0.632		
ichnofabric type 6	0.230		0.496		
organic carbon	-0.255	-0.233		0.725	0.255
warm water planktonic foraminifera	0.324		0.289	0.475	
$\delta^{13}\text{C}$ <i>Globigerinoides trilobus</i>			0.140	0.366	0.555
diversity benthic foraminifera	-0.214	-0.275	-0.556	-0.149	-0.196
oxyphylic foraminifera	-0.443	-0.424	-0.550		

Table 3a-c: **a** — Factor extraction based on maximum likelihood method and oblimin rotation with Kaiser normalization. **b** — Factor pattern matrix after oblimin rotation showing important factor loadings. **c** — Factor structure matrix after oblimin rotation showing important factor loadings.



Table 3d: Correlation matrix between factors.

Factor	1	2	3	4	5	6
1	1	0.352	0.541	0.053	-0.203	-0.067
2	0.352	1	0.188	-0.285	0.077	-0.099
3	0.541	0.188	1	0.235	0.086	-0.398
4	0.053	-0.285	0.235	1	0.147	-0.274
5	-0.203	0.077	0.086	0.147	1	-0.131
6	-0.067	-0.099	-0.398	-0.274	-0.131	1

ratios for *U. grilli* in the upper part of the section is confirmed by large variations (SD of 0.31) around 0.562 (Fig. 3d). The negative correlation between $\delta^{13}\text{C}$ and magnetic susceptibility in the upper part of the section as found with few measurements by *H. elegans* is also manifested by *U. grilli* (Table 2).

Oxygen isotope differences

Stratification of water masses can be estimated by the difference in $\delta^{18}\text{O}$ ($\Delta\delta^{18}\text{O}$; Báldi 2006) between *G. trilobus* and the benthic *U. grilli* (Fig. 3e). The lacking measurements of *U. grilli* in the deeper core can be replaced by the transformation

$$\delta^{18}\text{O}_{\text{grilli}} = \delta^{18}\text{O}_{\text{elegans}} - 0.582, n = 6.$$

Because differences between $\delta^{18}\text{O}$ at the warmer sea surface and the colder bottom are negative, absolute values were used (Fig. 3e). The weak but significant decrease ($b = -0.006$) in the lower part of the section indicates tendency toward poorly stratified water, starting with differences of 2.96 at 102 m declining to 2.59 at 40 m. Variations around the linear regression are weak (residuals: 0.219). These variations do not correspond to periods in magnetic susceptibility (Table 2). The opposite tendency in $\Delta\delta^{18}\text{O}$ can be seen in the upper part of the section. There, the variability increase is more than double ($b=0.017$) that of the lower part of the section ending with $\Delta\delta^{18}\text{O}=3.35$ at 8 m. This indicates intensification of water stratification in the younger sediments (Fig. 3e). Variability around the regression line is similar to that in the lower part of the section (residuals: 0.209). Also, in the upper part of the section, $\Delta\delta^{18}\text{O}$ oscillations do not correspond to variations of magnetic susceptibility (Table 2).

Ichnofossils

The cores, having been cut vertically, were examined for ichnofossils at 25 cm intervals (376 samples). Twelve ichno-species were identified (Pervesler et al. 2008). The ichnotaxa *Phycosiphon*, *Nereites* and *Thalassinoides* provide information about environmental conditions on the paleo-sea bottom. *Phycosiphon* predominates throughout the entire sequence, accompanied by major occurrences of *Nereites* (Pervesler et al. 2008). Both taxa represent pioneers that burrow in sediments with high amounts of particulate food and

oxygenated pore water. After an increased import of particulate organic matter, the deposit feeders producing *Phycosiphon* and *Nereites* are the first settlers (Wetzel & Uchmann 2001). They live entirely within the sediment and require oxygen rich pore waters as they horizontally rework the sediment. *Nereites* becomes less abundant when food content is reduced or when bottom conditions are more stable favouring ichnotaxa with burrows opening to the sea floor, such as *Thalassinoides*, *Chondrites*, *Trichichnus* and *Zoophycos* (Pervesler et al. 2008).

The average proportions of two ichnofabric types described in Pervesler et al. (2008) provide more information about the paleoenvironment. In the first ichnofabric type (Type 6 in Pervesler et al. 2008), *Nereites*, depending on well-oxygenated sediments, crosses *Phycosiphon* living at the same level. In the second ichnofabrics type (Type 1 in Pervesler et al. 2008), *Thalassinoides*, which characterizes stable bottom conditions at a higher level, crosses both *Phycosiphon* and *Nereites* burrows (Pervesler et al. 2008). The ichnofabric type with abundant *Nereites* does not show significant trends (Table 1) but demonstrates variations corresponding to those of magnetic susceptibility (Table 1; Fig. 4a). In the deeper part of the section (bottom to 68 m), the *Thalassinoides* ichnofabric is completely lacking. It appears and reaches a maximum between 60 m and 55 m, then decreases to 40 m (Fig. 4b). Periodic less frequent appearances in the upper part of the section correlate negatively with magnetic susceptibility (Table 2; Fig. 4b).

Benthic foraminifera

Benthic foraminifera were investigated in 74 samples taken throughout the section at 1.2 m spacing. 102 taxa could be distinguished (Báldi & Hohenegger 2008). The life style and distribution of benthic foraminifera allows further inferences about the paleoenvironment of the sea floor (e.g. Jorissen 1999; Murray 2006).

Inbenthic foraminifera

All species, which lead an inbenthic life today or extinct species for which an inbenthic life is inferred on the basis of morphological relations to living representatives, are summed and counted as a percentage of the total fauna (Báldi & Hohenegger 2008). Proportions of inbenthic foraminifera increase upward (Fig. 4c; Table 1). This increase is insignificant in the deeper part from 102 m to 40 m (Table 2) varying with a SD of 7.1 around the mean of 30.3 %. The significant increase in the upper part of the section (Table 3) starts with 35.5 % at 40 m reaching 44.2 % at the top. While negative correlations with magnetic susceptibility are insignificant in the deeper part of the section, they approach significance in the upper part (Table 2).

Oxyphytic foraminifera

Species belonging to this group (Báldi & Hohenegger 2008) need well-aerated bottom water reflecting an epibenthic or shallow inbenthic mode of life (e.g. Corliss

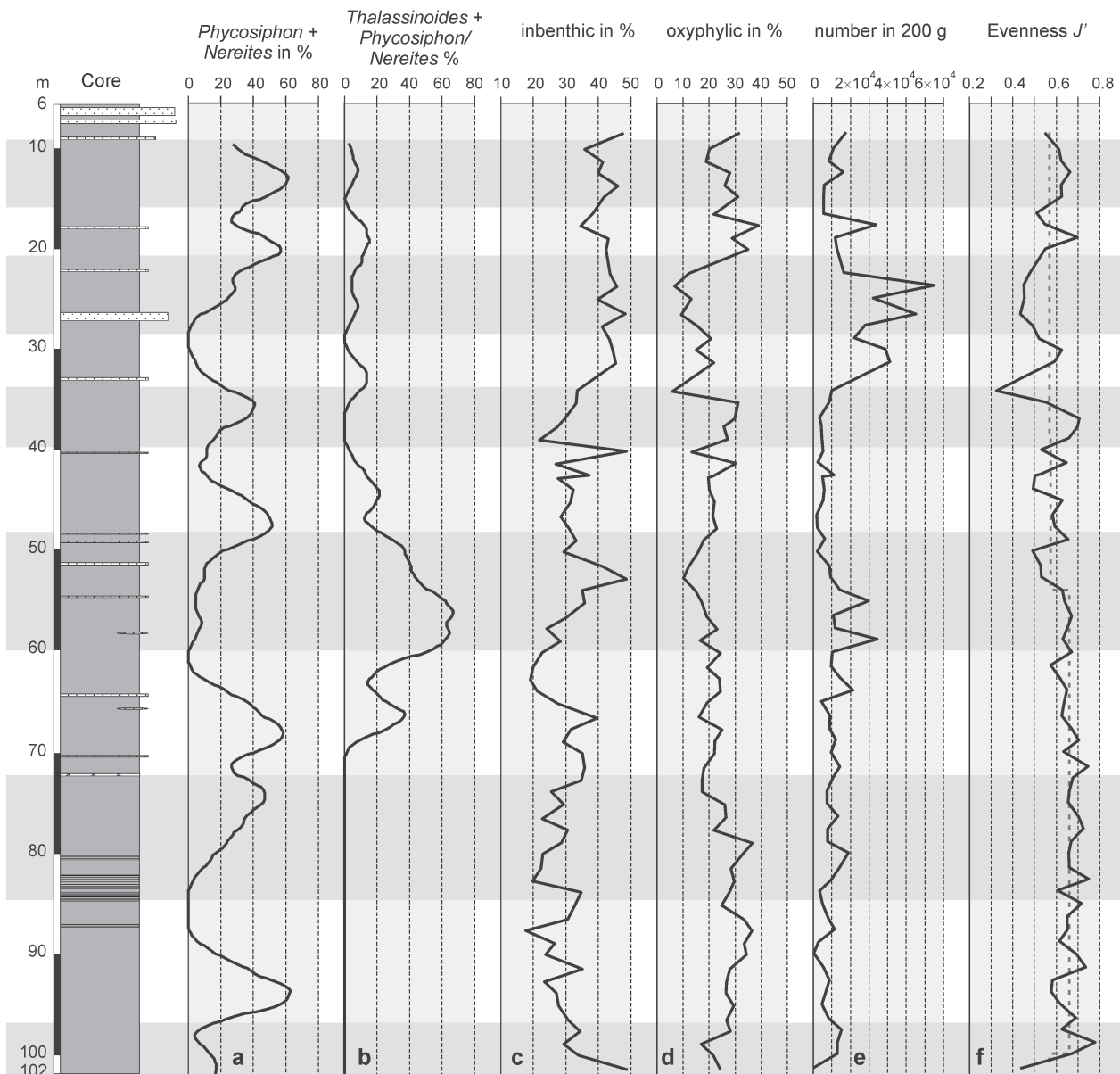


Fig. 4. **a** — Percentages of ichnofabric type 6 with *Phycosiphon* and *Nereites*. **b** — Percentages of ichnofabric type 1 with *Thalassinoides* crossing *Phycosiphon* and *Nereites*. **c** — Percentages of inbenthic foraminifera. **d** — Percentages of oxyphytic foraminifera. **e** — Abundance of benthic foraminifera. **f** — Diversity of benthic foraminifera. Grey and white bands indicate periods obtained by moving averages of magnetic susceptibility.

1991; Jorissen 1999). Percentages of oxyphytic foraminifera decrease from the bottom to the top of the section (Fig. 4d; Table 1). In the deeper part of the section, the significant decrease (Table 2) starts with 29.3 % at 102 m declining to 17.7 % at 40 m. Variations are weak (residuals: 5.2) correlating positively with magnetic susceptibility (Table 2). In the upper part of the section, percentages vary intensively ($SD=9.2$) around a mean of 22.0 %. These variations are positively correlated with magnetic susceptibility (Table 2).

Abundance

The benthic foraminiferal abundances were standardized for 200 g dry sediment (Báldi & Hohenegger 2008). High

abundance often reflects the dominance of a few species adapted to a specific habitat or dwelling in extreme habitats due to their opportunistic life; they can reproduce there unimpeded by interspecific competitors (e.g. Valiela 1995). The exponential growth in populations with unimpeded reproduction makes a logarithmic scale necessary to allow comparisons using linear statistical methods.

Abundance increases from the bottom to the top or the cored section, with a negative correlation to magnetic susceptibility (Fig. 4e; Table 1). The increase is insignificant in the deeper part (40 m to 102 m; Table 2), where abundance oscillates weakly ($SD=6.64 \times 10^3$) around a geometric mean of 7.34×10^3 individuals 200 g^{-1} . These variations are negatively correlated with magnetic susceptibility (Table 2). In

the upper part of the section, strong variations ($SD = 1.70 \times 10^4$) around a geometric mean of 1.35×10^4 individuals 200 g^{-1} are negatively correlated with magnetic susceptibility (Table 2). The significant increase in abundance from the bottom to the top of the sequence appears to be a stepwise function with mean values differing significantly between the lower and upper part of the section.

Diversity

In contrast to the high abundance that is often correlated with the dominance of a few species, diversity is characterized by numerous species possessing similar specimen abundances. Therefore, diversity is an indicator of habitat quality for the organism group (a discussion of the different factors causing diversity see Valiela 1995). From the various diversity measures, the Measure of Evenness (J'), derived from the Shannon Information Measure H' , was selected (Krebs 1989).

Diversity decreases significantly from the bottom to the top of the cored sequence (Fig. 4f; Table 1) exhibiting a positive correlation with magnetic susceptibility. The decrease is also significant in the deeper part of the section starting with $J' = 0.678$ at 102 m reaching $J' = 0.584$ at 40 m with weak variations (residuals: 0.096). Except the deepest sample, variations around a mean of $J' = 0.660$ are weak from 100 m to 53 m ($SD = 0.048$) suddenly intensifying ($SD = 0.063$) between 53 m and 38 m with a significantly lower mean of $J' = 0.571$ (Fig. 4f). Diversity variability is again more intensive in the upper part of the section (8 m to 40 m), with no significant relation to depth (Table 2). Again, the mean is lower ($J' = 0.564$) compared to the two lower intervals. Variations correlating with magnetic susceptibility (Table 2) have the highest amplitudes ($SD = 0.098$). Therefore, the significant decrease in diversity is not linear but is best explained by a stepwise function (Fig. 4f).

Planktonic foraminifera

This group of microorganisms can be used to evaluate conditions in the upper 500 meters of the pelagic realm. Planktonic foraminifera respond to many different environmental factors, but are mainly affected by temperature and nutrients (e.g. Hilbrecht 1996; Arnold & Parker 1999). Water depth is an important factor influencing the life cycles dependent on the depth of the thermocline, pycnocline, or the chlorophyll maximum (Arnold & Parker 1999).

Planktonic foraminifera were investigated from 36 samples taken at approximately 2.4 m intervals along the cored section (Rupp & Hohenegger 2008). They were grouped at the generic level or put into morphological groups such as 4-chambered or 5-chambered globigerinids. Beside the taxonomic investigation and their relationship to environmental factors, some indices and proportions characterizing the environment and/or environmental factors were measured.

Cold and cold-temperate water indicators

According to Hilbrecht (1996) and Li et al. (1999), higher abundances of "four- and five chambered globigerinids" as

well as *Turborotalita* signalize cold water, while *Globoturborotalita* and *Globorotalia* prefer cool-temperate water.

The high percentages of cold water planktonic foraminifera do not show a significant trend along the section (Table 1) oscillating with a standard deviation of 15.9 around a mean of 70.7 % (Fig. 5a). Variability is more intensive ($SD = 20.3$) in the upper core compared to the deeper part ($SD = 13.9$). In both parts of the stratigraphic sequence, the variations have a significant negative correlation with magnetic susceptibility (Table 2).

Warm and warm-temperate water indicators

Orbulinids, *Globigerinoides* and *Globoquadrina* are regarded as warm water indicators, while *Globigerinella* prefers warm-temperate environments (Bicchi et al. 2003; Rupp & Hohenegger 2008).

In percentage abundance, this group behaves oppositely to the group indicating cold water masses (Fig. 5b). This is evident in the high negative correlation between the two groups (Table 1). Relations of warm water indicators to depth in the section are insignificant for the entire sequence (Tables 1, 2). From 102 m to 40 m, percentages vary little ($SD = 11.4$) around a mean of 22.7 %. Variations become greater ($SD = 14.7$) in the upper part of the section around a lower mean of 15.9 %. In contrast to the cooler water indicators, the percentages of warm water planktonic foraminifera correspond positively to periods of increased magnetic susceptibility (Table 2).

Abundance

The planktonic foraminiferal abundances were standardized for 1 g dry sediment (Rupp & Hohenegger 2008). Because of the exponential growth in populations, logarithms of numbers were used for further linear statistical analyses.

Abundance declines from the bottom to the top of the sequence (Table 1) but these relations are insignificant in both the deeper and upper part of the section (Table 2). While mean abundance is high between 52 m and 102 m (geometric mean: $493.0 \text{ individuals g}^{-1}$ with a SD of 267.1), abundance is low from 52 m to 8 m (geometric mean: $189.7 \text{ individuals g}^{-1}$ with a significantly higher SD of 310.3 caused by a maximum of $1100 \text{ individuals g}^{-1}$ at 30 m; Fig. 5c). The decline in abundance can be explained by a stepwise function with different means (Fig. 5c). Negative correlations with magnetic susceptibility are significant for both the lower and the upper parts of the section (Table 2).

Diversity

Diversity of the planktonic foraminifera was calculated using the Simpson Index 1-D (D = Dominance; Rupp & Hohenegger 2008). Similarly to benthic foraminifera, the diversity of planktonic foraminifera is the opposite of abundance, as shown by the high negative correlation between both indices (Table 1). These correlations are not as high as for benthic foraminifera because diversity is constant throughout the entire sequence (regression coefficient $b = 7E-05$; Table 1) while abundance decreases. Evaluation of the increase

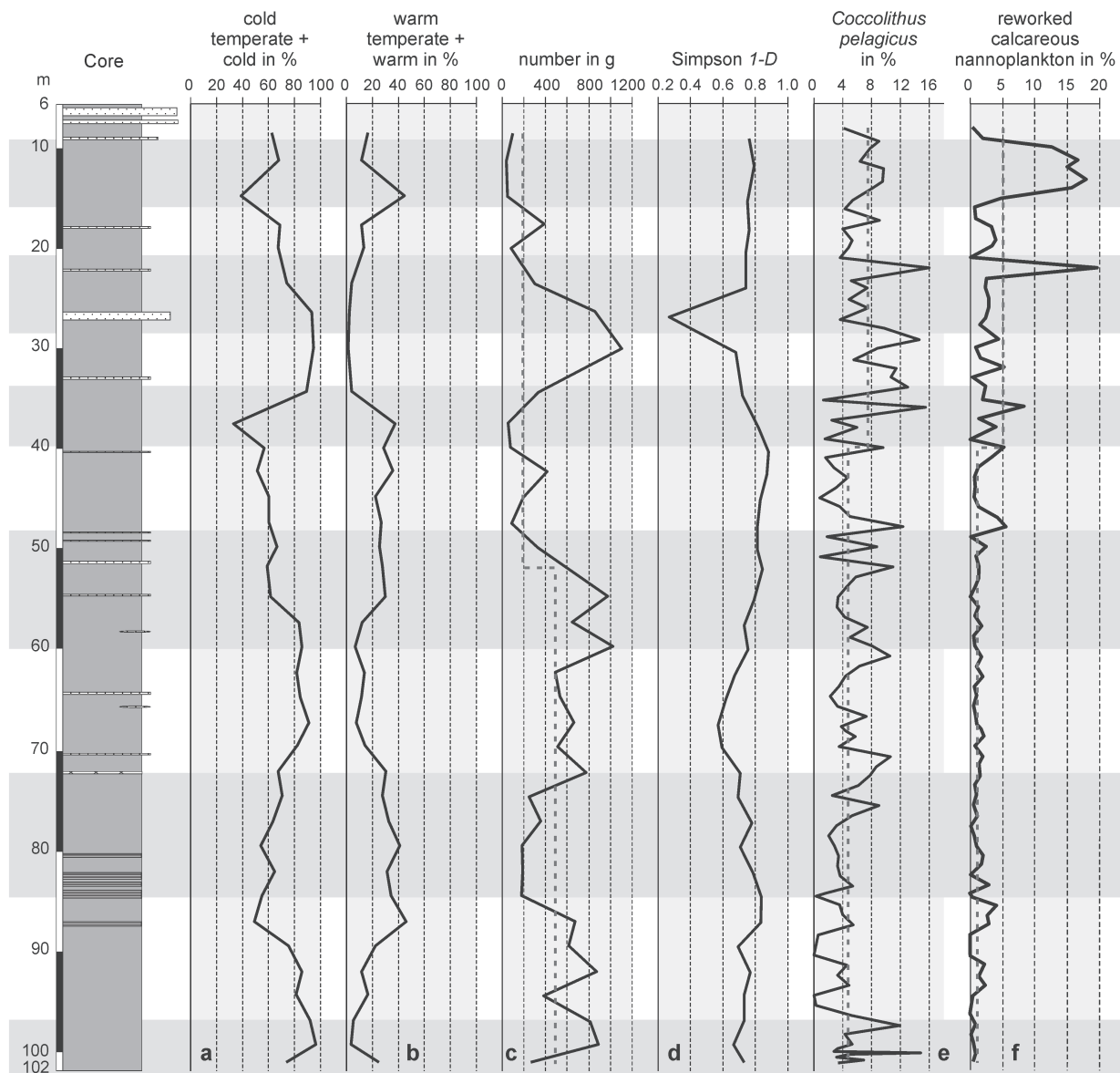


Fig. 5. **a** — Percentages of cold and cold temperate planktonic foraminifera. **b** — Percentages of warm and warm temperate planktonic foraminifera. **c** — Abundance of planktonic foraminifera. **d** — Diversity of planktonic foraminifera. **e** — Percentages of the nannoplankton *Cocolithus pelagicus*. **f** — Percentages of reworked nannoplankton. Grey and white bands indicate periods obtained by moving averages of magnetic susceptibility.

in plankton diversity is hampered by an extreme outlier at 26 m ($1-D=0.25$; Fig. 5d). Deleting the outlier from the analysis improves measure of the increase ($b=0.0006$), but it still remains insignificant. Diversity increases significantly ($b=0.0017$) in the deeper part of the section starting with 0.699 at 102 m and reaching 0.804 at 40 m (Fig. 5d) with residuals of 0.077. Neglecting the outlier at 26 m, diversity varies with standard deviations of 0.055 around a mean of 0.764. Correlation with magnetic susceptibility is significant throughout the whole section (Table 1).

Calcareous nannoplankton

Samples for the investigation of calcareous nannoplankton were taken at approximately 1 m spacing down to 100 m (94

samples). Seven additional samples were taken in ~20 cm intervals between 100 m and 102 m (Ćorić & Hohenegger 2008). Percentages of dominant species were used for characterizing assemblages and their dependence on environmental factors. Two groups with strong relations to environmental factors were analyzed, supporting the results obtained from planktonic foraminifera.

Cocolithus pelagicus

Cocolithus pelagicus is an important paleoecologic indicator. It is abundant in cold water (Okada & McInyre 1979; Winter et al. 1994). High proportions of this species also indicate higher nutrient levels and eutrophic conditions (Ćorić & Hohenegger 2008).

The proportion of *C. pelagicus* increases from the bottom to the top of the section (Table 1; Fig. 5e). In the deeper part of the section (40 m to 102 m) the increase is insignificant (Table 2), where proportions vary ($SD = 3.14$) around an average of 4.71 %. Between 8 m and 40 m, percentages are more variable ($SD = 3.82$) around a higher mean of 7.43 % (Fig. 5e). The significant increase of *C. pelagicus* along the sequence is thus not linear, but follows a stepwise function (Fig. 5e). Correlations with magnetic susceptibility are negative and significant in the deeper part of the section, but insignificant in the upper part (Table 2).

Reworked nannoplankton

Late Cretaceous, Paleogene and Early Miocene taxa indicate reworking of older sediments due to tectonic movement or increased erosion (Ćorić & Hohenegger 2008).

The proportion of reworked nannofossils increases significantly from the bottom to the top of the section, and is positively correlated with magnetic susceptibility (Table 1). This is in contrast to *C. pelagicus*, which is negatively correlated with magnetic susceptibility. Similar to the latter, an increase is insignificant in both parts of the sequence (Table 2). Percentages vary slightly ($SD = 1.18$) around 1.2 % in the deeper part of the section, becoming more variable ($SD = 5.62$) around a higher mean of 5.05 % in the upper part (Fig. 5f). Again, the increase over the entire section is not linear but can be explained with a stepwise function (Fig. 5f).

Environmental factors

To explain the factors that influenced the environmental variables explained above, we used the statistical methods summarized as ‘Latent Structure Models’ (Krzanowski & Marriott 1995), often termed ‘Factor Analysis’ (Davis 2002).

We used the ‘Maximum Likelihood Factor Analysis’, first developed by Lawley (1940), because it avoids many problems arising by other factor analytical methods (for details see Krzanowski & Marriott 1995; Davis 2002). After finding the optimum solution of independent factors explaining the frequency distribution of variables, these artificial mathematical factors can be interpreted as natural environmental factors. However, the independence of natural factors in environmental science as postulated by orthogonal factors, even though rotated, is unsustainable. For example, productivity of phytoplankton depends on non-stratified water masses, temperature and other parameters. Therefore, an oblique factor rotation optimizes the correlation between variables and factors that is expressed in the ‘structure matrix’. It also optimizes the correlation between factor loadings and the correlation matrix of variables expressed in the ‘pattern matrix’. By this process, factors are no longer independent but inter-correlated to different degrees. The ‘direct oblimin method’ (Jenrich & Sampson 1966) with Kaiser normalization was used here to get oblique (correlated) factors.

Previous calculations of factor analyses based on principal component extraction demonstrated that the variable ‘water

depth’ is a single factor. Therefore, this variable was excluded from the analysis. Before starting factor analysis, all percentage data were linearized by the arcsine-root transformation (Parker & Arnold 1999) and abundance data transformed to logarithms.

Five factors explaining 70 % of total variance were extracted and rotated for optimizing relations between variables and factors as well as optimizing correlations between factors (Table 3a). Factor loadings of variables are shown in the pattern and structure matrix (Table 3b,c). Factor scores for variables were calculated using the regression method.

In the following, five significant factors (eigenvalue > 1) are explained by their loadings and are interpreted in terms of ecology.

Factor 1

The main factor, initially explaining 30.6 % of total variance, and increasing to 34.9 % after oblique rotation (Table 3a), is most positively loaded by the variables ‘cold water planktonic foraminifera’, ‘abundance of planktonic foraminifera’ and ‘calcium carbonate content’, with additional positive loading by ‘organic carbon content’ and ‘differences in $\delta^{18}\text{O}$ between planktonic and benthic foraminifera’. High negative loadings are from ‘diversity of planktonic foraminifera’, ‘magnetic susceptibility’, ‘reworked nannoplankton’ and ‘warm water planktonic foraminifera’, with lesser negative loadings by ‘ichnofabric type 6 with *Nereites*’ and ‘oxyphylic benthic foraminifera’ (Table 3b,c).

This factor represents the mean temperature of the sea without differentiation between surface and bottom waters. This interpretation is supported by the dependence of the above variables on temperature. Beside direct temperature indicators such as warm and cold water foraminifera, the higher amount of calcium carbonate partly results from abundant planktonic foraminifera preferring nutrient-rich cold water combined with organic carbon originating from marine photosynthetic organisms. The negative loading by magnetic susceptibility confirms the correlation between terrigenous input through intensified weathering and erosion at times of maxima in eccentricity and obliquity, which led to higher insolation and increased seasonal differences. The higher input of terrigenous material during warm periods also explains the negative loading of reworked nannofossils for this cold-water factor. Factor scores, indirectly scaling paleo-temperature of the seawater during deposition, can now be used to demonstrate temperature changes in the time interval during which the sediments were deposited (Fig. 6). Periods of colder water were from 101 m to 92 m, from 73 m to 50 m and from 35 m to 23 m, while in the other intervals warm water dominated (Fig. 6).

Factor 2

This factor, initially explaining 14.5 % of total variance, becomes less important (3.2 %) after oblique rotation (Table 3a). Two opponents with extreme loadings characterize this factor. $\delta^{18}\text{O}$ of the planktonic foraminifer *G. trilobus* positively loads this factor, while ‘differences in $\delta^{18}\text{O}$ between planktonic and

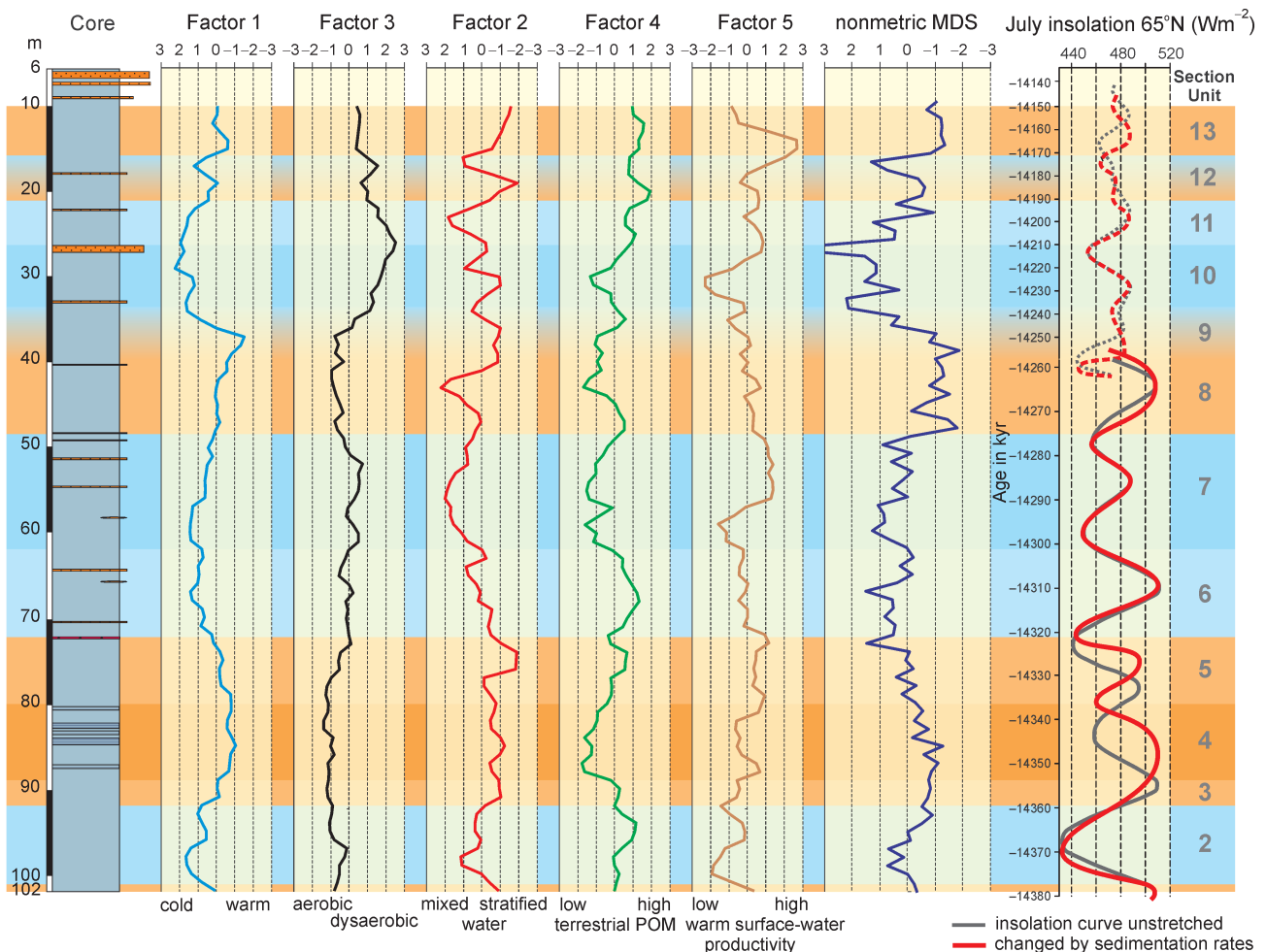


Fig. 6. Comparing factor scores obtained by maximum likelihood factor analysis with the single scale of nonmetric multidimensional scaling (MDS) and insolation curves between -14.379 and -14.142 Myr. Colors of the units indicate ‘warm’ (orange) and ‘cold’ (blue) temperatures.

benthic foraminifera’ shows high negative loadings (Table 3b,c). ‘Ichnofabric 1 with *Thalassinoides*’ has a high positive factor loading, while lower but significant positive loadings by $\delta^{18}\text{O}$ of the benthic *H. elegans*’ and ‘diversity of planktonic foraminifera’ additionally characterize this factor.

The extreme loading by positive $\delta^{18}\text{O}$ in both the planktonic and benthic foraminifers and the high negative loading in the $\Delta\delta^{18}\text{O}$ values allows the interpretation of this factor as a signal for stratified water masses. Positive scores indicate non-stratified, mixed water, while negative scores are typical of stratified water masses (Fig. 6).

The relation between Factors 1 and 2 demonstrate the advantage of oblique rotated factors. Both are positively correlated (Table 3d) confirming the correspondence between stratification and warm surface water. Differences between both factors show that water mixing occurred during warm water periods (Fig. 6). The intensive variation of this factor between 10 m and 40 m is partly caused by more intense environmental changes, but the incomplete stratigraphic record resulting from loss of sediments through tectonics must also be considered (Hohenegger et al. 2008; Ćorić & Hohenegger 2008).

Factor 3

The importance of the third factor, with an initial variance proportion of 12 % increasing to 24.1 % after oblique rotation approximates the Factor 1 (Table 3a). Factor 3 is high positively loaded by a series of variables starting with ‘ $\delta^{13}\text{C}$ of *H. elegans*’ and followed in decreasing order by ‘inbenthic foraminifera’, ‘abundance of benthic foraminifera’, ‘percentages of *C. pelagicus*’ and ‘ $\delta^{18}\text{O}$ of *H. elegans*’ (Table 3b,c). Lower positive loadings are by ‘differences in $\delta^{18}\text{O}$ between planktonic and benthic foraminifera’ and ‘ichnofabric 1 with *Thalassinoides*’. ‘Warm water planktonic foraminifera’, ‘oxyphytic benthic foraminifera’ and ‘diversity of benthic foraminifera’ load this factor negatively (Table 3b,c).

According to the positive and negative loadings, this factor seems to scale dysoxic bottom conditions. The main argument is based on the richness of inbenthic foraminifera coupled with their abundance, while diversity of benthic foraminifera is low. The indication of oxygen-depleted bottom sediments is supported by the negative loading of oxyphytic benthic foraminifera and the positive loadings by the trace

fossil *Thalassinoides* that prefers stable bottom conditions with burrows opening to the sea floor. Therefore, factors scores can be used as a scale measuring the intensity of oxygen depletion.

Again, this factor indicating the degree of oxygen depletion is highly positively correlated with Factor 1, which characterizes cold water, and less, but still significantly positively correlated with Factor 2 indicating the degree of stratification of the water (Table 3d). Using factor scores, oxygen depletion increases from the bottom to the top of the section, partially mimicking oscillations found in the temperature Factor 1 (Fig. 6).

Factor 4

Representing 7.8 % of the initial variance, the importance of this factor decreases to 3.3 % after rotation (Table 3a). The main variable loading this factor is ‘ichnofabric type 6 with *Nereites*’ followed in decreasing importance by ‘organic carbon content’, ‘ $\delta^{18}\text{O}$ of *H. elegans*’, ‘ $\delta^{18}\text{O}$ of *G. trilobus*’, ‘ $\delta^{13}\text{C}$ of *G. trilobus*’, ‘oxyphylic benthic foraminifera’, ‘cold water planktonic foraminifera’ and ‘reworked nannoplankton’ (Table 3b,c). This factor is weakly negatively loaded by ‘warm water planktonic foraminifera’, ‘diversity’ and ‘abundance of planktonic foraminifera’ (Table 3b,c).

This factor clearly indicates the input of particulate terrigenous organic material (POM) that is relatively rich in oxygen (type III kerogen) during periods of colder water. These produce the ideal environment for the opportunistic ichnofossil *Nereites*. Therefore, factor scores as a scale characterize the input of oxygen-rich particulate organic matter from land (Fig. 6).

Factor 5

The importance of this factor with a proportion of 5.8 % of the initial variance does not significantly decrease after oblique rotation (4.7 %). Two variables, ‘warm-water planktonic foraminifera’ and ‘ $\delta^{13}\text{C}$ of *G. trilobus*’, load this factor positively, accompanied by ‘differences in $\delta^{18}\text{O}$ between planktonic and benthic foraminifera’ and ‘ $\delta^{18}\text{O}$ of *H. elegans*’ (Table 3b,c). ‘Cold-water planktonic foraminifera’, accompanied with ‘abundance of planktonic foraminifera’ and ‘reworked nannoplankton’, cause negative loadings.

This factor reflects surface productivity, indicated by the high $\delta^{13}\text{C}$ of the shallow dwelling *G. trilobus*, a species that prefers warm water coupled with a high degree of stratification (Table 3b,c). These dependencies of Factor 5 explain the significant negative correlation to the temperature Factor 1 characterizing cold-water masses (Table 3d). Using factor scores as scales, variations of the temperature factor are weakly negatively mirrored by the productivity Factor 5 (Fig. 6).

Paleoenvironmental interpretation

Relating the numerical factors obtained by latent structure analysis to the main environmental parameters influencing

the distribution of organisms in the sea enables reconstruction of the environment in the Paratethys of the southern Vienna Basin and its changes during the late Early Badenian between -14.379 and -14.142 Myr. This precise dating (Hohenegger et al. 2008) allows evaluation of the variation of insolation, e.g. intensity of the sunlight that depends on orbital cycles during this time. Using Laskar et al. (2004), we calculated the insolation for summer months at 65° N for the time interval represented by the Baden-Sooss section to determine whether they can explain the changes in environmental conditions in the Badenian Sea on the southwestern border of the Vienna Basin. Although the environment changed continuously, the sequence could be partitioned into stratigraphic units deposited under similar conditions. These units are discussed in detail below (Fig. 6).

Unit 1 (101 m to 102 m; -14.379 Myr to -14.377 Myr)

The environment during deposition of the deepest part of the section can be reconstructed as fully marine with water depth around 300 m. In spite of warm temperatures and well-stratified water masses, oxygen depletion of the sediment was not extreme. The input of terrigenous particulate organic material rich in oxygen as well as the export productivity from the surface waters remained at a medium level (Fig. 6). The trace fossil *Trichichnus* indicating firm bottom reacted to the decreased input of oxygen, and high proportions of inbenthic foraminifera are explained through the dysaerobic conditions. Surface waters were characterized by abundant warm-water planktonic foraminifera (*Globigerinella*, *Globocyclina*) and the calcareous nannoplankton assemblage with warm-water indicators *Reticulofenestra* and *Sphenolithus*.

Unit 2 (92 m to 101 m; -14.377 Myr to -14.359 Myr)

The temperature decreased during this interval, reaching a minimum around 97 m, afterwards returning to mean temperatures at 93 m. This parallels the insolation curve as well as the signal for stratified water masses (Fig. 6). Both factors, cold and non-stratified water do not lead to major changes in oxygenation. On the contrary, moderate dysoxia at the beginning of this interval decreased continuously until its end. This decline can be explained by the rise in oxygen-rich particulate organic material. Increasing bottom instability is mirrored in the proportion of the *Nereites* dominated ichnofabric type 6. Additionally, the number of inbenthic foraminifera decrease continuously while oxyphylic taxa become important. Among planktonic foraminifera, the “five-chambered globigerinds” and *Turborotalita* indicate cold non-stratified water masses as does the nannoplankton species *Coccolithus pelagicus*.

Unit 3 (89 m to 92 m; -14.359 Myr to -14.353 Myr)

This is a short transitional interval. Temperatures remained at a medium level. Stratification and surface productivity increased together with a decline in terrigenous oxygen-rich organic material. Ichnofabric type 3 with *Scoli-*

cia replaced *Trichichnus* of the previous period suggesting a higher sedimentation rate (Pervesler et al. 2008) in this unit. A few laminated layers are visible (Wagreich et al. 2008). Higher sedimentation rates are also indicated by the magnetic susceptibility (Fig. 2a). Percentages of inbenthic foraminifera decreased, while oxyphylic forms increased slightly. *Globorotalia* dominated the planktonic foraminifera, with lower proportions of the warm-water *Globigerinoides*.

Unit 4 (80 m to 89 m; -14.353 Myr to -14.344 Myr)

This unit is characterized by abundant mm thick laminations, especially between 82 m and 85 m (Wagreich et al. 2008) and high magnetic susceptibility (Fig. 2a). The temperature was warm and conditions became the most oligotrophic of the entire section. During the times of maximum lamination, the waters were well oxygenated and the input of terrigenous oxygen-rich particulate organic matter reached a minimum (Fig. 6). The lamination, partly destroyed by the opportunistic *Phycosiphon*, can be explained by the higher sedimentation rates impeding bioturbation (Pervesler et al. 2008).

Dating of the sequence indicates a mean sedimentation rate of 470 mm/kyr for the deeper, tectonically unaffected part (Hohenegger et al. 2008). Distances of ~1 mm between the dark lamellae in the main laminated part at 84.5 m correspond to an annual sedimentation rate of 1000 mm/kyr, roughly doubling the ‘normal’ sedimentation rate, and is reflected in the peak in magnetic susceptibility (Fig. 2a). Stretching the insolation curve to correct for the higher sedimentation rate, shows a maximum corresponding to the peak in temperature (Fig. 6). Oxyphylic benthic foraminifera are abundant and the proportion of inbenthics is low (Fig. 4c,d). The planktonic foraminifer *Globorotalia* dominates throughout the unit, indicating waters deeper than 240 m. This genus is accompanied in the lower and upper part of the unit by *Globigerinoides* and in the strongly laminated central part of the unit by the warm-water indicators *Globigerinella* and *Globoquadrina* (Rupp & Hohenegger 2008). *Globigerinoides* and *Globigerinella* are abundant in the transition to the succeeding unit 5. *Reticulofenestra minuta* dominates the calcareous nannoplankton, sometimes accompanied by *Sphenolithus*. Beside these warm-water indicators, *Umbilicosphaera jafarii*, characteristic for warm and slightly hypersaline water, makes its first appearance (Ćorić & Hohenegger 2008).

Unit 5 (73 m to 80 m; -14.344 Myr to -14.323 Myr)

This interval marks a transition from warm to cooler water conditions (Fig. 6). Declining temperature is coupled with an increase in eutrophication (Fig. 6). The input of oxygen-rich particulate organic material is high, thus the ichnofabric type with *Nereites* needing oxygen rich sediments dominates. At the end of this interval, bottom conditions become more oxygen depleted as indicated by *Zoophycus* and *Scolicia* (Pervesler et al. 2008). The increase in eutrophication is also documented in the decline of oxyphylic and the increase of inbenthic foraminifera (Fig. 4c,d). The planktonic foraminifi-

fer *Globorotalia* dominates the whole unit, where *Globigerinoides* has its maximum in the deeper part and is abundant up to the end of the interval (Rupp & Hohenegger 2008). *Coccolithus pelagicus* indicating non-stratified cooler water becomes more common than in the previous unit, while the warm water species *R. minuta* decreases. The abundant *U. jafarii* as an additional warm-water species hint to the less cooling during this interval (Ćorić & Hohenegger 2008).

Unit 6 (62 m to 73 m; -14.323 Myr to -14.301 Myr)

Together with the subsequent unit, this interval is characterized by low but constant terrestrial sediment input as indicated by magnetic susceptibility (Fig. 2a). Temperature continues the decline that started in the previous period, while eutrophication perpetuates at a medium level (Fig. 6). Water mass changes from well- to non-stratified water and the input of oxygen-rich particulate organic material remains high, while shallow water productivity weakens during this interval. During high oxygen-rich input of particulate organic material, the ichnofabric type with *Nereites* dominates. Decrease of this input in the uppermost part leads to dysoxic bottom conditions and the first *Thalassinoides* ichnofossil appears (Fig. 4b). The proportion of inbenthic foraminifera is high in the deeper part and decreases towards the upper part, whereas oxyphytic taxa are of low to medium abundance (Fig. 4d). *Globorotalia* reaches its highest proportions in this unit, and along with “four-chambered globigerinids” dominates the planktonic foraminifera. The nannoplankton *U. jafarii* reaches its highest proportion in this unit. Reticulofenestrids are of medium abundance, while the proportion of *C. pelagicus* is high, but not extreme, confirming the cooler conditions during this interval (Ćorić & Hohenegger 2008).

Unit 7 (49 m to 62 m; -14.301 Myr to -14.275 Myr)

Temperature cools to a local minimum at 58 m, afterwards rising slightly to a medium level at 50 m. This tendency is also pictured in a distinct lack of stratification of the water mass. Oxygen depletion reaches a maximum at 52 m that is the highest for the deeper, tectonically unaffected part of the section (Fig. 6). This maximum coincides with a peak in shallow-water productivity, whereas the input of particulate organic material gets a minimum. Ichnofabric type 1 with *Thalassinoides*, which prefers dysoxic bottom conditions shows its highest proportions during this period (Pervesler et al. 2008). Inbenthic foraminifera increase to a maximum at 53 m, where a minimum in oxyphytic species is observed (Fig. 4d). The slightly increasing input of oxygen-rich particulate organic material at the end of this unit, which is also marked by an increment of coarse-grained sediments (Wagreich et al. 2008), leads to higher abundance of the benthic foraminifer *Trifarina angulosa*, which prefers well-aerated, turbulent bottom water (Báldi & Hohenegger 2008). Colder water planktonic foraminifera dominate in the lower part of the interval, but their abundance decrease, when warm-water planktonic foraminifera like *Globigerinella* and *Globoquadrina* become abundant (Fig. 5a,b; Rupp & Hohenegger 2008). Dominance of the nannoplankton *R. minuta*, abundant *C. pelagicus* together with the complete lack of *Sphenolithus* indicate medi-

um water temperature and lower salinity (Ćorić & Hohenegger 2008). The latter is additionally documented by the benthic foraminifer *Trifarina angulosa* (Báldi & Hohenegger 2008).

Unit 8 (38 m to 49 m; -14.275 Myr to -14.258 Myr)

The temperature increased during this interval. This tendency is correlated with a trend toward oligotrophic conditions. Although temperatures were high, the increased stratification of the water mass is interrupted at 43 m. This is also reflected in a lower input of particulate organic material. The sea bed sediments were oxygen depleted at the beginning of the interval, characterized by ichnofabric type 1 with *Thalassinoides*, but later became oxygenized as a result of increased terrigenous input indicated by a maximum of magnetic susceptibility (Fig. 2a). *Nereites* becomes the dominant ichnofossil in the younger interval. After the strong increase of inbenthic foraminifera in the previous interval, a slight decline in their abundance between 42 m and 49 m is followed by a large increase at the end (Fig. 4c). The benthic foraminifer *T. angulosa* is abundant in the lower part (Báldi & Hohenegger 2008) but decreases towards the end. The proportion of the warm water planktonic foraminiferal genera *Globigerinoides*, *Globigerinella* and *Globigerinata* increases (Rupp & Hohenegger 2008). Dominance of the nannoplankton *R. minuta* together with fewer sphenolithids indicates the warm water and euryhaline conditions in the upper part of the unit (Ćorić & Hohenegger 2008).

Unit 9 (35 m to 38 m; -14.258 Myr to -14.237 Myr)

The first major tectonic disturbances can be seen in the lower part of this unit, between 35 m and 37 m (Wagreich et al. 2008). They are indicated by a strong decrease in magnetic susceptibility at the beginning of the period separating it from the previous interval. Environmental conditions changed rapidly. The temperature increased to a maximum at 37 m and suddenly changes back to colder at the end of the interval. Oxygen depletion shows the opposite trend and the input of particulate organic material follows the same trend. Stratification of the water column was initially high but decreased suddenly with sinking temperatures (Fig. 6). Shallow water productivity continued to decrease. Magnetic susceptibility is high, indicating intensified input of terrigenous material. Laminations also suggest an increased sedimentation rate. Thus, bottom conditions are similar to the middle part of unit 4 between 82 m and 85 m. The opportunistic ichnofossil *Phycosiphon* dominates (ichnofabric type 4; Pervesler et al. 2008) and *Nereites* becomes abundant at the end of this interval. The proportion of inbenthic foraminifera is low at the beginning and increases rapidly until the end of the interval. *Trifarina angulosa* declines until the end of this period, reaching ‘normal’ proportions there (Báldi & Hohenegger 2008). After a maximum of colder water planktonic foraminifera at the beginning of the interval, warm-water genera like *Globigerinoides*, *Globigerinella* and *Globigerinata* become abundant but are replaced at the end by colder water “five-chambered globigerinids” (Rupp & Hohenegger 2008). Environmental changes are also mirrored

in calcareous nannoplankton. The colder water indicator *C. pelagicus* marks the beginning and the end of the interval accompanied by >5 % reworked nannoplankton, the warm-water indicators *R. minuta* and *S. heteromorphus* are abundant during the middle part of the unit. The normally rare *S. heteromorphus* reaches its highest abundance (>3 %) in the entire sequence (Ćorić & Hohenegger 2008).

Unit 10 (27 m to 35 m; -14.237 Myr to -14.210 Myr)

An approximately 50 cm thick conglomerate layer is developed between 27.2 m and 27.7 m and significant tectonic faults are visible between 29 m and 30 m and at 35 m (Wagreich et al. 2008: Appendix 1B,C). Magnetic susceptibility is lower than in the previous period, but there is intense variability correlated with high terrestrial input at the beginning and end of the interval. The temperature declined sharply with a minimum at the end, and the waters became more dysoxic (Fig. 6). The water column varied between non-stratified and weakly stratified and the input of terrigenous particulate organic material as well as surface productivity reached a local minimum at 30 m (Fig. 6). The laminations from the previous period continue, but disappear in the middle of the unit to return and increase again towards the end (Wagreich et al. 2008). Ichnofabric type 4, with the pioneer *Phycosiphon* crossing the lamellae, is frequent at the bottom and at the top of the unit, whereas the weakly-stabilized bioturbated bottom sediment of the lower part of the unit show ichnofabric type 6 with *Nereites*. This was later replaced by ichnofabric type 1 dominated by *Thalassinoides* characterizing firm bottom conditions. Proportions of inbenthic foraminifera increase reaching maximum percentages at the end of the period, while oxyphylic species are rare. Oxygen depletion during the later part of this interval is also manifested in the deep infaunal species *Bolivina elongata*. It reaches an abundance maximum of 30 % at 27 m (Báldi & Hohenegger 2008: fig. 3a). Colder water “five-chambered globigerinids”, *Globorotalia* and “four-chambered globigerinids” constitute >90 % of planktonic foraminifera (Rupp & Hohenegger 2008: figs. 2, 4). The abundance of the colder water nannoplankton species *C. pelagicus* is highest in this unit, where peak occurrences coincide with non-stratified water masses (Fig. 5e). Abundant reticulofenestrids indicate more stratified water in the middle part and at the end of the period (Ćorić & Hohenegger 2008).

Unit 11 (21 m to 27 m; -14.210 Myr to -14.192 Myr)

The upper two meters of this unit are strongly affected by tectonics (Wagreich et al. 2008: Appendix 1B). The magnetic susceptibility is highly variable, suggesting varying terrigenous input. The temperature increased from a minimum at the beginning of the interval to a more moderate level at the end. Oxygen depletion decreased after an initial maximum (Fig. 6). The initially non-stratified water mass tends towards weak stratification with a sharp return to non-stratified conditions at 22 m. Input of particulate organic material increased while that from shallow productivity remained moderate; both decline sharply at 22 m (Fig. 6). Ichnofabric

types also change from laminations overprinted by *Phycosiphon* (ichnofabric type 4 in Pervesler et al. 2008) to pure *Nereites*-dominated sediments (ichnofabric type 5_2 in Pervesler et al. 2008), then to dysoxic bottom conditions as characterized by *Thalassinoides* (ichnofabric type 1). The proportion of inbenthic foraminifera remains high, between 40 and 50 %, whereas oxyphylic taxa show low percentages (Fig. 4c,d). The deep infaunal species *Bolivina elongata* reaches its second maximum of 30 % at 22.5 m, then decreases upwards (Báldi & Hohenegger 2008). Colder water planktonic foraminifera, especially the “five-chambered globigerinids”, *Globigerinata* and *Globoturborotalita*, which dominated the previous unit decrease slightly. The warm-water indicator *Globigerinoides* reappears in extremely low proportions at the end of the interval. The incomplete record of planktonic foraminifera resulting from the large sample spacing cannot resolve the break in the other environmental variables at 22 m. The better record of calcareous nannoplankton clearly demonstrates this change with *C. pelagicus*, attaining maximum abundance (16 %) at 22 m and by the highest proportion (20 %) of reworked nannofossils (Ćorić & Hohenegger 2008).

Unit 12 (16 m to 21 m; -14.192 Myr to -14.171 Myr)

Magnetic susceptibility is the lowest within the upper part of the section between 8 m and 40 m, but variability is high indicating major changes in terrigenous input. The temperature increases slightly from medium to high, then decreases rapidly at 17 m. This is also documented by the change from highly stratified to weakly stratified waters at 19 m (Fig. 6). Oxygen depletion becomes intense at 17 m. Input of terrigenous particulate organic material is high and shallow productivity tended to a maximum. The opportunistic ichnofossils *Phycosiphon* and *Nereites* dominate during this period after initial presence of *Thalassinoides* (Pervesler et al. 2008). Inbenthic foraminifera are dominated by *Bolivina viennensis* but are slightly less abundant than in the preceding unit. Proportions of oxyphylic species increase rapidly, but this may be caused through reworking and transport from shallower regions (Fig. 4d). The decrease in colder water planktonic foraminifera continues, with a minimum of 40 % at 16 m, while warm water foraminifera, especially *Globigerinoides*, increase to a maximum of 40 % at the same depth (Fig. 5a,b). The lower temperature of the water at 17 m depth is mirrored by the increase of the nannoplankton species *C. pelagicus*. Reworked nannoplankton indicate input from the land (Ćorić & Hohenegger 2008).

Unit 13 (? 8 m; 10 m to 16 m; -14.171 Myr to -14.149 Myr)

After a strong increase at the beginning of the unit, magnetic susceptibility attained the third maximum peak along the section at 14 m (Fig. 2a) followed by a decrease to 8 m (Fig. 2a). Temperatures remained constantly high, similar to the input of terrigenous particulate organic material. In contrast to the usual opposite behaviour between temperature and oxygen depletion, the latter remains high during this interval. Water masses were well stratified. Shallow water pro-

ductivity was extremely high at the bottom of the unit but decreased rapidly upwards. The well-oxygenized sea floor was favourable for ichnofabric type 6 with *Nereites*, *Thalassinoides*, *Scolicia* and *Trichichnus* characterized oxygen depleted bottom conditions at the end of the interval (Pervesler et al. 2008). Percentages of inbenthic foraminifera are always high, around 40 %, but increase considerably from 10 m to 8 m (Fig. 4c). Oxyphylic benthic foraminifera parallel the trend in inbenthics, but this could be caused by transport from shallower regions (Báldi & Hohenegger 2008). This is also supported by the extremely high proportion of reworked nannoplankton. During this interval, the cold water planktonic foraminifera suddenly decrease at 14 m replaced by warm water planktonic genera. This change is also marked by the dominance of the warm water nannoplankton species *U. jafarii* at 14 m replacing the high proportions of the colder water indicator *C. pelagicus* elsewhere (Ćorić & Hohenegger 2008).

Conclusion

The stratigraphic sequence cored at Baden-Sooss allows reconstruction of the paleoenvironment and changes during the late Early Badenian, just prior to the time the stratotype sediments of the Badenian were deposited. The position of the locality on the southwestern border of the small Vienna Basin close to the Alpine landmass complicates the paleoceanographic interpretation, which is traditionally based on proxies and variables typical of the open ocean. For instance, stable oxygen isotopes cannot be used as paleotemperature indicators in the Badenian Sea of the Vienna Basin because of the varying salinities caused by the freshwater input from nearby landmasses and because the restricted Vienna Basin had only narrow connections to the larger water body of the Pannonian Sea (Kováč et al. 2004; Strauss et al. 2006). The shape and depth of the basin, together with the opening and closing of connections to the Pannonian Sea/Paratethys, influenced both the shallow and deep water circulation (Colling 2001). Stratification of the water mass has to be interpreted carefully. The few measurements of Ca/Mg-ratios of the aragonitic foraminifer *Hoeglundina elegans* indicate bottom water temperatures around 16.5 °C at water depths estimated to be between -250 m and -300 m for the older part of the section, declining to 14 °C in the upper part, which was deposited in water depths between -200 m and -250 m. Although differences in the uptake of Mg between species and even within a single specimen (Toyofuku & Kitazato 2006) hamper precise estimations, the slight temperature differences between surface planktonic and benthic foraminifera in stratified water are significant.

Stratification became somewhat better developed during deposition of the upper strata. The middle of the thermocline would be expected to be much deeper than the sea bottom at this locality. The thermocline was probably fully developed only in the center of the basin.

Evidence from the base of the section at 102 m (-14.379 Myr) indicates high water temperatures and stratified water masses. Both parameters decrease to a minimum

at 97 m (-14.368 Myr), then increase constantly upward. The cooler period between 92 m and 100 m corresponds to the insolation minimum between -14.376 and -14.360 Myr (Laskar et al. 2004). Although temperatures were low, the slightly disaerobic conditions at 102 m intensify, then become more oxic again. Percentages of oxyphylic benthic foraminifera, colder water planktonic foraminifera and the cold water nannoplankton species *Coccolithus pelagicus* all increase upward. Producers of the ichnofossils *Phycosiphon* and *Nereites* sought particulate organic material rich in oxygen as food, and reworked the sediment.

Between 73 m and 92 m (-14.357 Myr to -14.344 Myr) the evidence suggests high temperatures. Magnetic susceptibility is high, and the sediment input double the normal sedimentation rate, i.e. from around 400 mm/kyr to ca. 1000 mm/kyr. The insolation curve shows two prominent peaks between -14.360 and -14.300 Myr that could have been responsible for strong seasonal changes causing higher weathering rates and sediment input, while the weak trough between insolation peaks had little influence on the main environmental trend. The higher sedimentation rate is indicated not only by the maxima in magnetic susceptibility, but also by the increased input of reworked nannoplankton and by abundant, partly undisturbed 1 mm sediment laminations. Due to the well-stratified water, the deeper waters were oxygen depleted, and the proportion of inbenthic foraminifera becomes the lowest of the entire section, but increases at the end of this interval. Oxyphylic benthic foraminifera are abundant along with warm water planktonic foraminifera (*Globigerinoides*) and calcareous nannoplankton (reticulofenestrids, sphenolithids). Bottom sediments were more prone to bioturbation at the beginning and at the end of this unit. Conditions were optimal for the pioneers *Phycosiphon* and *Nereites*. *Phycosiphon* was able to reoccupy the laminated central part of this unit. Other ichnofossils were excluded due to the high sedimentation rate.

Sedimentation rates were low and steady during deposition of the strata between 49 m and 73 m (-14.344 Myr to -14.301 Myr), as indicated by the slight variability of magnetic susceptibility. Low temperatures induced oxygen depletion. A temperature increase started at 52 m (-14.280 Myr) and continued into the following periods. This 'cool' period is divided into two parts, paralleling the insolation curve. Stratification of the water masses decreased accompanied by a peak in accumulation of particulate organic material. The minima of both variables can be found in the middle of the overlying unit around 56 m. Due to the stable bottom conditions with low oxygen, the ichnofossil *Thalassinoides*, which produced burrows with openings, appeared in the lower part of this unit and became abundant in the upper part. Proportions of inbenthic foraminifera are high. Colder water planktonic foraminifera such as "five-chambered globigerinids" and *Globorotalia*, and the nannoplankton species *C. pelagicus* dominate during this interval. Higher sedimentation rates and low salinity at the end of this period are indicated by absence of *Sphenolithus* and by presence of the inbenthic foraminifer *Trifarina angulosa*.

The overlying 'warm period' between 38 m and 49 m (-14.301 Myr to -14.275 Myr) is the last tectonically unaffected section in the core. It contains the second maximum of

terrestrial sedimentary input as documented by magnetic susceptibility. This is suddenly interrupted by tectonic deformation between 36 m and 38 m. Temperatures were highest during this period, but oxygen depletion was lower than in the previous interval, remaining at moderate level. Water mass stratification was interrupted around 43 m (-14.264 Myr) by mixing. Oxygenation of the bottom waters is reflected in the higher proportion of oxyphylic benthic foraminifera. The ichnofossil *Nereites* is abundant, while in the water column warm-water planktonic foraminifera and nannoplankton are abundant.

The upper part of the section is tectonically disturbed leading to a 43 % loss of the stratigraphic record (Hohenegger et al. 2008). Comparison with the insolation curve becomes more difficult. A major rapid cooling can be reconstructed between 35 m and 38 m (-14.258 Myr to -14.237 Myr), then slowing to reach a minimum temperature around 26 m (-14.211 Myr). Oxygen depletion shows the opposite trend reaching a maximum at the same depth. Both environmental factors tend to an average level at 21 m (-14.192 Myr). Stratification of the water varied strongly during this interval and the proportion of inbenthic foraminifera is high. The abundance of all benthic foraminifera becomes the highest of the entire sequence. Due to changing bottom conditions, *Nereites* dominates the ichnofauna alternating with *Thalassinoides*. Planktonic foraminifera are almost exclusively colder water forms, while the nannoplankton *C. pelagicus* is abundant.

The youngest strata from 8 m to 21 m (-14.192 Myr to -14.142 Myr) are characterized by the third maximum of magnetic susceptibility corresponding to an insolation maximum. Extreme amounts of reworked nannoplankton document higher sediment input. Temperature is relatively high and oxygen depletion, normally opposite to temperature, remains at an elevated level. The proportion of inbenthic foraminifera is also higher compared to the earlier warm-water periods. The proportion of pelagic cold-water indicators like *C. pelagicus* remains higher than in other warm-water periods, whereby alternations with the warm-water, higher salinity indicator *Umbilicosphaera jafarii* suggest apparently rapid environmental changes, but this may be a reflection of the discontinuous sedimentary record.

The tectonic deformation of this part of the section produces artificially rapid changes by interrupting otherwise continuous sedimentation. Stronger oscillations of magnetic susceptibility in the upper part of the section compared to the lower part, together with the increased input of sediment indicated by the reworked nannoplankton and shallow water benthic foraminifera as well as by the coarse-grained material (sands and conglomerates), documents the greater tectonic activity during deposition of the younger strata.

General trends during deposition of the sequence are declining temperatures and increasing oxygen depletion. The only effect of the slight shallowing from -260 m to -240 m water depth was on the decreasing abundance of a few deep dwelling planktonic foraminifera (e.g. *Globorotalia*).

The precise dating of the core between -14.379 and -14.142 Myr allows correlation of the environmental changes with the global paleoclimate (e.g. Zachos et al. 2001; Shevenell et al. 2004; Holbourn et al. 2007) taking into ac-

count the position of the Badenian Sea as a marginal basin separated from the main Paratethys through sills. Therefore, periods with higher temperatures in the deeper part of the sequence led to strong differences between the mixed surface layer and the upper thermocline during summer, while these differences became weaker in winter. During 'cooler' periods, temperature differences between surface and bottom waters were not so strong in summer and extremely weak in winter, and vertical transport of nutrients was not hindered by density differences. This is indicated by the higher plankton productivity during cold periods, leading to peaks in organic carbon and calcium carbonate content.

The cooling tendency between \sim 14.7 and \sim 13.9 Myr (Phase 2 in Holbourn et al. 2007 after the Middle Miocene 'Monterey' carbon isotope excursion), when these sediments were deposited, was mainly controlled by global climatic factors. Low orbital eccentricity and obliquity led to enhanced organic burial, as can be shown by the higher $\delta^{13}\text{C}$ ratios of *Hoeglundina elegans* and *Globigerinoides trilobus* (Fig. 3c,d). Enhanced organic burial favoured atmospheric CO_2 drawdown and global cooling. When insolation variations were minimal, as during the time of deposition of the upper core, the ocean-climate system became more susceptible to CO_2 changes (Berger & Loutre 2003). Strong oscillations in the upper part of the section can be explained by the fluvial input due to 'cooler' weather, i.e. stronger physical erosion in the hinterland, together with tectonic movements that brought coarser material into the basin.

The paleoenvironment of the Baden-Sooss core was controlled primarily by varying insolation intensities depending on orbital cycles. Seasonal changes strongly influenced temperature and stratification of the water mass in the marginal sea of the Vienna Basin. The general trend to lower temperatures and increased oxygen depletion of the deeper waters follows global climate changes, intensified or weakened by local paleogeographic conditions.

Acknowledgments: The study was supported by the Projects P13743-BIO, P13740-GEO and P16793-B06 of the Austrian Science Fund (FWF). We thank Maksuda Khatun, Fred Rögl, Anna Selge and Karl Stingl, coworkers in these projects, for their help and discussion. Further thanks are due to Maria Fencl, Wilfried Körner, Robert Scholger, Alfred Uchman and Inge Wimmer-Frey for cooperation in various respects. Special thanks are due to William W. Hay, who critically commented the manuscript and improved the English text.

References

- Abdul Aziz H., Di Stefano A., Foresi L.M., Hilgen F.J., Iaccarino S.M., Kuiper K.F., Lirer F., Salvatorini G. & Turco E. 2008: Integrated stratigraphy and $^{40}\text{Ar}/^{39}\text{Ar}$ chronology of early Middle Miocene sediments from DSDP Leg 42A, Site 372 (Western Mediterranean). *Palaeogeogr. Palaeoclimatol. Palaeoecol.* 257, 123–138.
- Arnold A.J. & Parker W.C. 1999: Biogeography of planktonic Foraminifera. In: Sen Gupta B.K. (Ed.): Modern Foraminifera. *Kluwer Academic Publishers*, Dordrecht, 103–122.
- Báldi K. 2006: Paleoceanography and climate of the Badenian (Middle Miocene, 16.4–13.0 Ma) in the Central Paratethys based on foraminifera and stable isotope ($\delta^{18}\text{O}$ and $\delta^{13}\text{C}$) evidence. *Int. J. Earth Sci. (Geol. Rdsch.)* 95, 119–142.
- Báldi K. & Hohenegger J. 2008: Paleoecology of benthic foraminifera of Baden-Sooss section (Badenian, Middle Miocene, Vienna Basin, Austria). *Geol. Carpathica* 59, 5, 411–424.
- Bemis B.E., Spero H., Bijma J. & Lea D.W. 1998: Reevaluation of the oxygen isotopic composition of planktonic foraminifera: experimental results and revised paleotemperature equations. *Paleoceanography* 13, 150–160.
- Berger A. & Loutre M.-F. 2003: Climate 400,000 years ago, a key to the future. In: Droxler A.W., Poore R.Z. & Burckle L.H. (Eds.): Earths climate and orbital eccentricity: The marine isotope stage 11 question. *Geophys. Monogr. Ser. 137, Amer. Geophys. Union*, Washington, DC, 17–26.
- Bicchi E., Ferrero E. & Gonera M. 2003: Paleoclimatic interpretation based on Middle Miocene planktonic Foraminifera: the Silesia Basin (Paratethys) and Monteferraro (Tethys) records. *Palaeogeogr. Palaeoclimatol. Palaeoecol.* 196, 265–303.
- Chiessi C.M., Ulrich S., Multizzi S., Pätzold J. & Wefer G. 2007: Signature of the Brazil-Malvinas Confluence (Argentine Basin) in the isotopic composition of planktonic foraminifera from surface sediments. *Mar. Micropaleontology* 64, 52–66.
- Cicha I., Papp A., Senes J. & Steininger F.F. 1975: Badenian. In: Steininger F.F. & Nevesskaya L.A. (Eds.): Stratotypes of Mediterranean Neogene stages. 2. *VEDA*, Bratislava, 43–49.
- Colling A. (Ed.) 2001: Ocean circulation. The open University. *Butterworth & Heinemann*, Milton Keynes, UK, 1–286.
- Corliss B.H. 1991: Morphology and habitat preferences of benthic foraminifera from the northwest Atlantic Ocean. *Mar. Micropaleontology* 17, 195–236.
- Ćorić S. & Hohenegger J. 2008: Quantitative analyses of calcareous nannoplankton assemblages from the Baden-Sooss section (Middle Miocene of Vienna Basin, Austria). *Geol. Carpathica* 59, 5, 447–460.
- Davis J.C. 2002: Statistics and data analysis in geology. *John Wiley & Sons*, New York, XVI+639 pp.
- Espitaliè J., LaPorte J.L., Madec M., Marquis F., Leplat P., Paulet J. & Bouteleau A. 1977: Méthode rapide de caractérisation des roches mères de leur potentiel pétrolier et de leur degré d'évolution. *Rev. Inst. Francaise Pétrole* 32, 23–42.
- Grossmann E.L. 1984: Stable isotope fractionation in live benthic foraminifera from the Southern California borderland. *Palaeogeogr. Palaeoclimatol. Palaeoecol.* 47, 301–327.
- Hammer O. & Harper D. 2005: Paleontological data analysis. *Blackwell Publishing*, Malden, MA, 1–351.
- Hilbrecht H. 1996: Extant planktonic foraminifera and the physical environment in the Atlantic and Indian Oceans. *Mitt. Geol. Inst. Eidg. Techn. Hochsch. Univ. Zürich, Neue Folge* 300, 1–93.
- Hohenegger J. 2005: Estimation of environmental paleogradient values based on presence/absence data: a case study using benthic foraminifera for paleodepth estimation. *Palaeogeogr. Palaeoclimatol. Palaeoecol.* 217, 115–130.
- Hohenegger J., Ćorić S., Khatun M., Pervesler P., Rögl F., Rupp C., Selge A., Uchman A. & Wagreich M. 2008: Cyclostratigraphic dating in the Lower Badenian (Middle Miocene) of the Vienna Basin (Austria) — the Baden-Sooss core. *Int. J. Earth Sci.* DOI 10.1007/s00531-007-0287-7.
- Holbourn A., Kuhnt W., Schulz M., Flores J.-A. & Andersen N. 2007: Orbitally-paced climate evolution during the middle Miocene "Monterey" carbon-isotope excursion. *Earth Planet. Sci. Lett.* 261, 534–550.
- Jennrich R.I. & Sampson P.F. 1966: Rotation for simple loadings. *Psychometrika* 32, 363–379.
- Jorissen F.J. 1999: Benthic foraminiferal microhabitats below the sediment-water interface. In: Sen Gupta B.K. (Ed.): Modern foramin-

- ifera. *Kluwer Academic Publishers*, Dordrecht, 161–179.
- Khatun M. 2007: Sedimentary petrology of Miocene (Badenian) sediments — comparison of the Southern Vienna Basin (Austria) and the Bengal Basin (Bangladesh). *Unpubl. PhD Thesis*, University of Vienna, 1–108.
- Kováč M., Baráth I., Harzhauser M., Hlavatý I. & Hudáčková N. 2004: Miocene depositional systems and sequence stratigraphy of the Vienna Basin. *Cour. Forsch.-Inst. Senckenberg* 246, 187–212.
- Krebs C.J. 1998: Ecological methodology. *Harper & Row Publishers*, New York, NY, XII + 654pp.
- Kroon D. & Darling K. 1995: Size and upwelling control of the stable isotope composition of *Neogloboquadrina dutertrei* (d'Orbigny), *Globigerinoides ruber* (d'Orbigny) and *Globigerina bulloides* d'Orbigny: examples from the Panama Basin and Arabian Sea. *J. Foram. Res.* 25, 39–52.
- Kruskal J.B. 1964: Nonmetric multidimensional scaling: a numerical method. *Psychometrika* 29, 115–131.
- Krzanowski W.J. & Marriott F.H.C. 1995: Multivariate analysis. Part 2. Classification, covariance structures and repeated measurements. *Arnold*, London, VIII + 280pp.
- Laskar J., Robulet P., Joutel F., Gastineau M., Correia A.C.M. & Levrard B. 2004: A long-term numerical solution for the insolation quantities of the Earth. *Astronomy & Astrophysics* 428, 261–285.
- Lawley D.N. 1940: The estimation of factor loadings by the method of maximum likelihood. *Proc. Roy. Soc. Edinburgh*, Ser. A60, 64–82.
- Li Q., James N.P., Bone Y. & McGowran B. 1999: Palaeoceanographic significance of recent foraminiferal biofacies on the southern shelf of Western Australia: a preliminary study. *Palaeogeogr. Palaeoclimatol. Palaeoecol.* 147, 101–120.
- Murray J.W. 2006: Ecology and applications of benthic foraminifera. *Cambridge University Press*, Cambridge, XI + 426pp.
- Okada H. & McIntrye A. 1979: Seasonal distribution of the modern Coccolithophores in the western North Atlantic Ocean. *Mar. Biology* 54, 319–328.
- Papp A. & Steininger F. 1978: Holostratotypus des Badenien. Holostratotypus: Baden-Sooss (südlich von Wien), Niederösterreich, Österreich. Badener Tegel-Keferstein, 1828 (Unterbaden; M4b; Obere Lagidenzone). In: Papp A., Cicha I., Senes J. & Steininger F. (Eds.): Chronostratigraphie und Neostratotypen: Miocän der Zentralen Paratethys. Bd. VI. M₄ Badenien (Moravien, Wieliczen, Kosovien). *VEDA SAV*, Bratislava, 138–145.
- Parker W.C. & Arnold A.J. 1999: Quantitative methods of data analysis in foraminiferal ecology. In: Sen Gupta B.K. (Ed.): Modern Foraminifera. *Kluwer Academic Publishers*, Dordrecht, 71–89.
- Pervesler P., Uchman A. & Hohenegger J. 2008: New methods for ichnofabric analysis and correlation with orbital cycles exemplified by the Baden-Sooss section (Middle Miocene, Vienna Basin). *Geol. Carpathica* 59, 5, 395–409.
- Rohling E.J. & Cooke S. 1999: Stable oxygen and carbon isotopes in foraminiferal carbonate shells. In: Sen Gupta B.K. (Ed.): Modern foraminifera. *Kluwer Academic Publishers*, Dordrecht, 239–258.
- Rupp C. & Hohenegger J. 2008: Paleoecology of planktonic foraminifera from the Baden-Sooss section (Middle Miocene, Badenian, Vienna Basin, Austria). *Geol. Carpathica* 59, 5, 425–445.
- Selge A. 2005: Cyclostratigraphy by means of mineral magnetic parameters in the middle Badenian (Middle Miocene) core Soob / Baden (Vienna Basin, Austria). *Unpubl. Diploma Thesis*, University of Leoben, 1–84.
- Sharp Z. 2007: Principles of stable isotope geochemistry. *Pearson Prentice Hall*, Upper Saddle River, NJ, XII + 344pp.
- Shepard R.N. 1962: The analysis of proximities: multidimensional scaling with an unknown distance function. I and II. *Psychometrika* 27, 125–139, 219–246.
- Shevenell A.E., Kennett J.P. & Lea D.W. 2004: Middle Miocene Southern Ocean cooling and Antarctic cryosphere expansion. *Science* 305, 1766–1770.
- Spero H.J. & Lea D.W. 1996: Experimental determination of stable isotope variability in *Globigerina bulloides*: implications for paleoceanographic reconstructions. *Mar. Micropaleontology* 28, 231–246.
- Strauss P., Harzhauser M., Hinsch R. & Wagreich M. 2006: Sequence stratigraphy in a classic pull-apart basin (Neogene, Vienna Basin). A 3D seismic based integrated approach. *Geol. Carpathica* 57, 185–197.
- Toyofuku T. & Kitattzato H. 2006: Mg/Ca micro-distribution in foraminiferal tests — implication of laboratory culture experiments. *Anuário do Instituto de Geociências* 29–1, 469–470.
- Valiela I. 1995: Marine ecological processes (2nd edition). *Springer Verlag*, New York, XIV + 686pp.
- Van der Zwaan G.J., Jorissen F.J. & de Stigter H.C. 1990: The depth dependency of planktonic/benthic foraminiferal ratios: Constraints and applications. *Mar. Geol.* 95, 1–16.
- Wagreich M., Pervesler P., Khatun M., Wimmer-Frey I. & Scholger R. 2008: Probing the underground at the Badenian type locality: geology and sedimentology of the Baden-Sooss section (Middle Miocene, Vienna Basin, Austria). *Geol. Carpathica* 59, 5, 375–394.
- Wetzel A. & Uchman A. 2001: Sequential colonization of muddy turbidites: examples from Eocene Beloveža Formation, Carpathian, Poland. *Palaeogeogr. Palaeoclimatol. Palaeoecol.* 168, 171–186.
- Winter A., Jordan R. & Roth P. 1994: Biogeography of living coccolithophores in ocean waters. In: Winter A. & Siesser W. (Eds.): Coccolithophores. *Cambridge University Press*, Cambridge, 13–37.
- Zachos J., Pagani M., Sloan L., Thomas E. & Billups K. 2001: Trends, rhythms, and aberrations in global climate 65 Ma to Present. *Science* 292, 696–693.